Antenna diversity for digital video broadcasting

Janssen, J.G.W.M.

Award date:
1993

EINDHOVEN UNIVERSITY OF TECHNOLOGY

FACULTY OF ELECTRICAL ENGINEERING

TELECOMMUNICATIONS DIVISION EC

Antenna Diversity for Digital Video Broadcasting

by J.G.W.M. Janssen

Report of the graduation work, carried out from march 1993 until November 1993 at the Philips Research Laboratories in Eindhoven.

Supervisors: prof. dr. ir. G. Brussaard, ir P.F.M. Smulders and ir P.G.M. de Bot (Philips).

Abstract

In the European dTTb[1] project, a transmission scheme for a new digital terrestrial TV system is under development. This scheme uses the OFDM[2] technique to divide the wide-band channel into a large number of narrow-band subchannels. Guard intervals are used to combat Inter-Symbol-Interference. The transmission scheme must allow indoor reception. With indoor/portable reception the received signal suffers from frequency selectivity. This means that a number of subchannels in the OFDM spectrum may be received very poorly. A widely used method of improving the received signal is to apply antenna diversity. More than one antennas are used to receive the signal. The received signals are combined in a combiner. The combiner improves the average signal-to-noise ratio and the distribution of the signal-to-noise ratio. Because of the little spatial variation of the wide-band received signal power for indoor reception, traditional wide-band combining will not result in much gain. In this report we analyze the performance of antenna diversity with narrow-band combining.

From one of the buildings of Philips Research labs in Eindhoven, an OFDM spectrum of 7 MHz is being transmitted. Measurements of the received spectrum have been carried out on different locations. Two antennas were used to measure the received spectra as a function of the distance between the two antennas. The measured spectra could be combined for each OFDM subchannel separately, using traditional combining techniques such as maximum ratio or selection combining. It is also possible to take a group of subchannels as being one in the combining process. With the aid of computer simulations, the performance improvement achieved with antenna diversity and a certain combining technique, could be calculated.

If we define the gain achieved with antenna diversity, to be the difference in required S/N ratio for a certain bit error rate with and without antenna diversity, we found an average gain of 7 dB when narrow-band maximum-ratio combining was used. Selection combining gave an average gain of 6 dB. Increasing the combining bandwidth resulted in a decrease of performance. Wide-band combining still resulted in an average gain of 2 dB. It was also found that the antenna spacing had to be larger than $\frac{\lambda}{3} = 13$ cm to receive sufficiently uncorrelated signals at both antennas, where λ is the wavelength of the transmitted signal.

Locations with poor reception conditions benefit even more from antenna diversity. With maximum-ratio combining, the average gain for these locations is 10 dB.

[1] Digital Terrestrial Television Broadcasting
[2] Orthogonal Frequency Division Multiplexing

Keywords

propagation, indoor reception, OFDM, fading, spatial selectivity, frequency selectivity, multipath reception, impulse response, antenna diversity, combining techniques narrowband combining

Preface

This report is the final report concluding the research work for the Master's degree in Electrical Engineering of the Eindhoven University of Technology. The research work is in the field communications engineering. The work is carried out at Philips Research in Eindhoven during the period March 1993-November 1993 and is related to the Digital Terrestrial Television Broadcasting (dTTb) project in which Philips participates.

To objective of this report is to find what improvement can be expected when antenna diversity is used in a dTTb-like transmission scheme. Chapter 2 describes such a dTTb-like transmission scheme. The theory of antenna diversity and some combining techniques are described in Chapter 3. The measurement setup is described in Chapter 4. In Chapter 5 the simulation results are presented for two different combining techniques. Some conclusions are drawn in Chapter 5. Finally, in Chapter 6 some directions for further research are given.

I would like to thank all those who helped me carrying out the research work and writing this report. Especially, I want to thank Ir P.G.M. de Bot and Ing. A.J.M. Wijlaars for coaching me during the last nine months are reviewing this report very thoroughly. Further, I thank Dr. Ir. C.P.M.J. Baggen for very thoroughly reviewing my previously written article. Further, I thank Prof. Dr. Ir. G. Brussaard and Ir. P.F.M. Smulders from the Eindhoven University of Technology for their assistance and for the opportunity they gave me to perform my graduation work with Philips. Finally, I would like to thank everybody at Philips Research who made my stay there pleasant.

Eindhoven, November 30, 1993

Johan G.W.M. Janssen

Contents

Chapter 1

Introduction

Philips Nat.Lab. participates in the European project Digital Terrestrial Television Broadcasting (dTTb). This project aims to design a digital television standard. This new digital television system should replace the current analog PAL/SECAM system. The plan is to introduce this new television system before the end of the century. This new digital system must supply a hierarchy of picture qualities, ranging from Standard Definition (SD) which is comparable with PAL quality via Enhanced Definition (ED) to High Definition (HD). One of the requirements of the new system is the feasibility of portable reception with a small built-in antenna.

A digital TV system can roughly be divided into three parts : Source Coding, Channel coding and Multiplexing. Source coding is concerned with the compression of the video/audio- information. Using MPEG-II based source coding, 5 Mbit/sec provides a SD video quality, 10 Mbit/sec ensures a virtual artifact free studio quality, called ED and 25 Mbit/s allows HD studio quality. Due to the limited availability of frequencies, the transmission must take place in the same channels as the current terrestrial television system (VHF bands 1 & 3 and UHF band 4 & 5). The bandwidth of the UHF channels is 8 MHz. This implies that the total bit-stream (video, audio, data), has to be transmitted over a channel having a bandwidth of 8 MHz. Due to the scarcity of the available spectrum and the increasing demand for a large variety of television programs, the system must allow as many programs in the available bandwidth as possible. Channel coding is concerned with the reliable information transmission from the transmitter to the receiver. Channel coding must supply portable/indoor reception of SD quality and fixed reception providing ED/HD quality. This implies that the system must be able to transmit the same program in more qualities (hierarchical transmission). From a channel coding point of view this is achieved by using a so called 2-resolution QAM signal constellation, in combination with error-correcting coding to combat the transmission impairments [9]. In Section 2.5 the 2-resolution signal constellation is described.

The terrestrial transmission channel is characterized by the effect of multipath propagation. Due to terrain conditions, mountains and buildings, the transmitted signal reaches the receiver through many different paths. Since these paths have different lengths, each path has its typical delay (echo). The echoes might introduce, in a digital communication system, Inter-Symbol-Interference (ISI). One way to combat ISI is to employ Orthogonal

Frequency Division Multiplexing (OFDM) with guard intervals. This technique is described in Section 2.3.

If a narrow-band signal is transmitted over a multipath channel, the received signal strength at the receiver will be very location dependent. By shifting the antenna over a short distance, the received signal strength might be very different.
If a wide-band signal (f.e. an OFDM signal) is transmitted over a multipath channel, the received signal will suffer from frequency selectivity. This means that the received signal strength will be dependent on the frequency. When the receiver is placed indoors, there will usually be no line-of-sight component in the received spectrum. This type of channel is often modeled by a Rayleigh channel model. Because of the frequency selectivity, some sub-channels can be in a deep fade, and data in these sub-channels will be unreliable.

One way to improve the transmission quality is to use more than one antenna (antenna diversity). Because of the frequency selectivity and the little variation of the wide-band received signal power, as a function of the antenna location, traditional wide band combining will not result in much gain. In [9], a new combining method is presented. This new combining method combines the received signals for each OFDM channel separately.

With the aid of measurements and simulations the performance improvement, using this new combining method, is calculated and presented. From one of the buildings of Philips Nat.Lab., an OFDM test signal is being transmitted. This test signal is used for channel measurements. How these measurements were carried out is explained in Chapter 4. With the results obtained from these measurements, simulations are carried out. In Chapter 5 the simulation results are presented, and we will see what performance improvement can be expected. Combining can not only be performed for each OFDM channel separately, but it is also possible to combine more than one channel at the same time. These results can be compared with sub channel and wide band combining.

Some preliminary results have previously been published in [16].

Chapter 2

Description of the transmission scheme

This chapter describes an example of the transmission scheme used in the dTTb project [9]. In this example we assume we can transmit 2 SD/ED programs per 8 MHz channel. For each program, we want to transmit 5 Mbit/s to portable receivers (SD) and additionally 5 Mbit/s to fixed receivers (ED). In the example, we use OFDM with guard intervals. The 2-resolution transmission is achieved by using a 2-resolution QAM signal constellation.In this example, Reed-Solomon coding gives burst error correction capability to combat the frequency selective nature of the transmission channel. The main components in this transmission scheme, such as the characteristics of the multipath channel and OFDM techniques are described in detail.

2.1 The transmission system

The transmission scheme used in this report is illustrated in Figure 2.1. The signal is transmitted over a channel with a bandwidth of 8 MHz. In this scheme a diversity combiner is included. This double antenna/front-end structure is a receiver option.

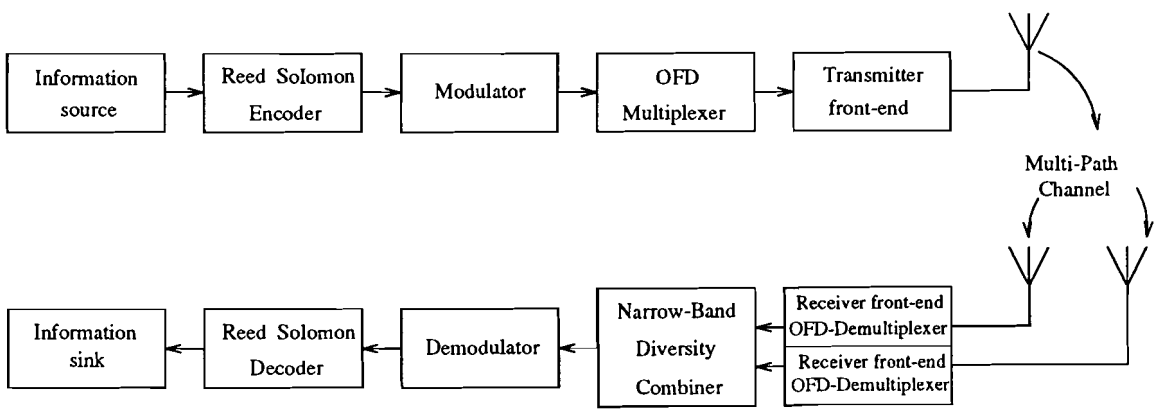

Figure 2.1: Implementation of the transmission scheme.

2.2 The Multipath Channel

In this section the multipath channel will be described briefly. We will look at this multipath channel in the time domain, in the frequency domain and in the space domain. Some assumptions will be made and we will see that a wide-band signal which is transmitted over a multipath channel will reach the receiver heavily disturbed. First the concept of fading will be explained as it is used a numerous times throughout this report.

2.2.1 Fading, Frequency selectivity & Spatial selectivity

In literature, the concept of fading is described often. Because in literature, the term fading is being used for many different effects, "fading" will be defined here as it is used throughout the rest of the report.

Traditionally, fading is linked to the time domain, i.e. the received signal strength varies as a function of time. This effect will further be called fading. In 'The New IEEE Standard Dictionary of Electrical and Electronics Terms', fading is defined as: The variation of radio field intensity caused by changes in the transmission medium, and transmission path, in time.
In this report the assumption is made that variation of the received radio field strength can also occur in the space domain and in the frequency domain. In the first case, the received signal strength is very location dependent, this effect is called spatial selectivity. If we suffer from variation in the frequency domain, this is called frequency selectivity. Frequency selectivity can occur at the receiver side when a wide-band signal is transmitted over a multi-path channel. Finally we introduce combined frequency and spatial selectivity. The received signal strength is not only dependent on the location of the receiver but also on the specific frequency we consider.

Throughout the rest of this report we assume a time-stationary channel, i.e. we don't suffer from fading.

2.2.2 Characteristics of the multipath channel in the time domain

The word multipath channel is self-explanatory. Literally this means that there is more then one path over which the transmitted signal travels before it reaches the receiver. If we transmit an extremely short puls $\delta(t)$ over a multipath channel, the received signal might appear as a train of pulses, as shown in Fig 2.2.

Each individual path has its own attenuation factor a_i and propagation delay τ_i. The impulse response $h(\tau)$ of the channel at delay τ can be described by

$$h(\tau) = \sum_{i=0}^{\mathcal{N}-1} a_i \delta(\tau - \tau_i), \tag{2.1}$$

where $\mathcal{N}$ is the number of paths between the transmitter and receiver. The attenuation factors a_i, the propagation delays τ_i and the number of paths $\mathcal{N}$ can be considered to be

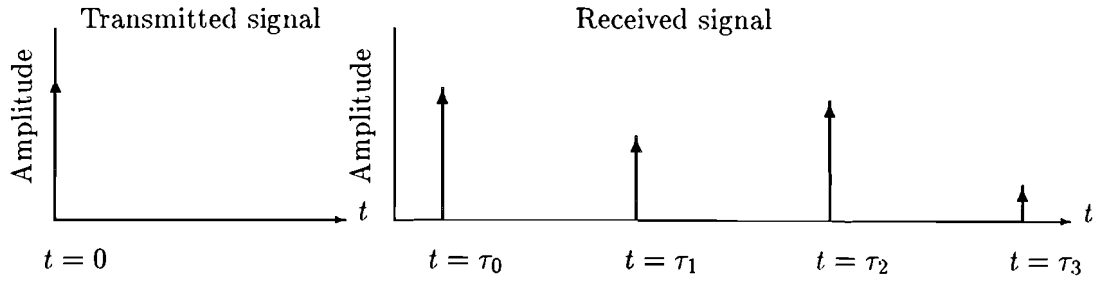

Figure 2.2: Example of the response of a multipath channel to an impulse

random variables that change with the antenna position.

Let us examine the effects of the channel on a transmitted signal that is represented by

$$s(t) = \sqrt{E_s} e^{j2\pi f_c t}. \tag{2.2}$$

The equivalent lowpass received signal can be described by

$$r(t) = \sum_{i=0}^{\mathcal{N}-1} a_i \, s(t - \tau_i) = \left(\sum_{i=0}^{\mathcal{N}-1} a_i e^{-j2\pi f_c \tau_i} \right) s(t) = \left(\sum_{i=0}^{\mathcal{N}-1} \alpha_i \right) s(t) = \alpha s(t), \tag{2.3}$$

where α is the resulting complex attenuation factor. Due to the central limit theorem, the resulting α will be complex Gaussian distributed for $\mathcal{N} \rightarrow \infty$. If the phases of the different signals add up destructively, this will result in a received signal that is very small or practically zero. On the other hand, when the different signals add constructively, the received signal amplitude will be larger. Thus the amplitude variations in the received signal, are due to the multipath characteristics of the channel.

When the complex attenuation factor α is a zero mean complex-valued gaussian variable, the envelope $|\alpha|$ can be described by a Rayleigh probability density function. In other words, there will be no line of sight component between transmitter and receiver. In this case the channel is said to be a *Rayleigh channel.* On the other hand, when there is a strong line of sight (or specular) component in the received signal, in addition to random scatters, α has no longer a zero mean. In this case, the envelope of $|\alpha|$ has a Rice distribution and the channel is said to be a *Ricean channel.* Finally, when all power is in the specular component the Ricean channel reduces to a Additive White Gaussian Noise (AWGN) channel. From the three channel types described, the Rayleigh channel is obviously the worst. The Rayleigh channel is often used as a model for the terrestrial broadcast channel with indoor reception.

In this treatment of transmission channels, only the Rayleigh channel is considered. In the presence of AWGN $n(t)$, the received signal becomes

$$r(t) = \alpha s(t) + n(t), \tag{2.4}$$

and the channel is characterized. If we make the assumption that τ_i is small with respect to the symbol duration, (2.4) becomes also valid for sinusoidal waves with information. In a digital transmission scheme the transmitted signal $s(t)$ can be selected from a set of possible waveforms

$$s(t) \in \{s_1(t), s_2(t), \cdots, s_M(t)\} \tag{2.5}$$

where

$$s_k(t) = \sqrt{E_{s_k}} e^{j(2\pi f_c t + \theta_k)} \tag{2.6}$$

and E_{s_k} is the envelope and θ_k is the phase information of the transmitted signal. When we represent the signal set $s_k(t)$ in the complex plane, where $\cos(2\pi f_c t)$ and $\sin(2\pi f_c t)$ are the two orthogonal bases [25], this becomes

$$s_k = \sqrt{E_{s_k}} e^{j\theta_k}. \tag{2.7}$$

The same transformation can be carried out with the AWGN $n(t)$. The relevant part of the AWGN becomes n in the complex plane. If we transmit signal s, the received signal r can now also be expressed in the complex plane and becomes

$$r = \alpha s + n. \tag{2.8}$$

From (2.8) it can be seen that the received signal-to-noise ratio equals $\gamma_s = \frac{\alpha^* \alpha E_s}{N_0}$ with $E[nn^*] = N_0$ and $E[ss^*] = E_s$. If we now assume that

$$E[\alpha\alpha^*] = 1, \tag{2.9}$$

the average received signal-to-noise ratio $\overline{\gamma}_s$ becomes $\overline{\gamma}_s = \frac{E_s}{N_0}$.

We shall now develop a useful correlation function that defines the characteristics of a multipath channel. Our starting point is the equivalent low-pass impulse response $h(\tau)$, where $h(\tau)$ denotes the response at delay τ. The attenuation factors and propagation delays of the different delay paths are assumed to be uncorrelated (*uncorrelated scattering*). Since $h(\tau)$ is wide-sense-stationary we can define the output power of the impulse response of the channel as

$$\phi_c(\tau) = h^*(\tau)h(\tau), \tag{2.10}$$

where $h^*(\tau)$ is the complex conjugate of $h(\tau)$. $\phi_c(\tau)$ is called *the delay power spectrum* of the channel [22].

An averaged function $\phi_c(\tau)$ is shown in Figure 2.3. The range of values of τ over which $\phi_c(\tau)$ is essentially nonzero is called the *multipath spread* of the channel and is denoted by T_m. Usually the scatterers are said to be essentially nonzero if their received power is less than 30 dB down with respect to the strongest path. The multipath spread T_m depends heavily on the environment. For rural and urban areas, we see typical multipath spread values of 0.7 μs respectively 7 μs [14].

2.2.3 The multipath channel in the frequency domain

The multipath channel can be characterized similarly in the frequency domain. By taking the Fourier transform of $h(\tau)$ we obtain the frequency transfer function $H(f)$. Because of the division of the wide-band channel into narrow subchannels, as will be described in Section 2.3, we are mainly interested in the channel behavior in the frequency domain. Each subchannel has its own attenuation factor α which can be described by a probability density function. The α values of adjacent subchannels are mutually correlated. An important measure for this correlation is the *coherence bandwidth* B_c of the channel.

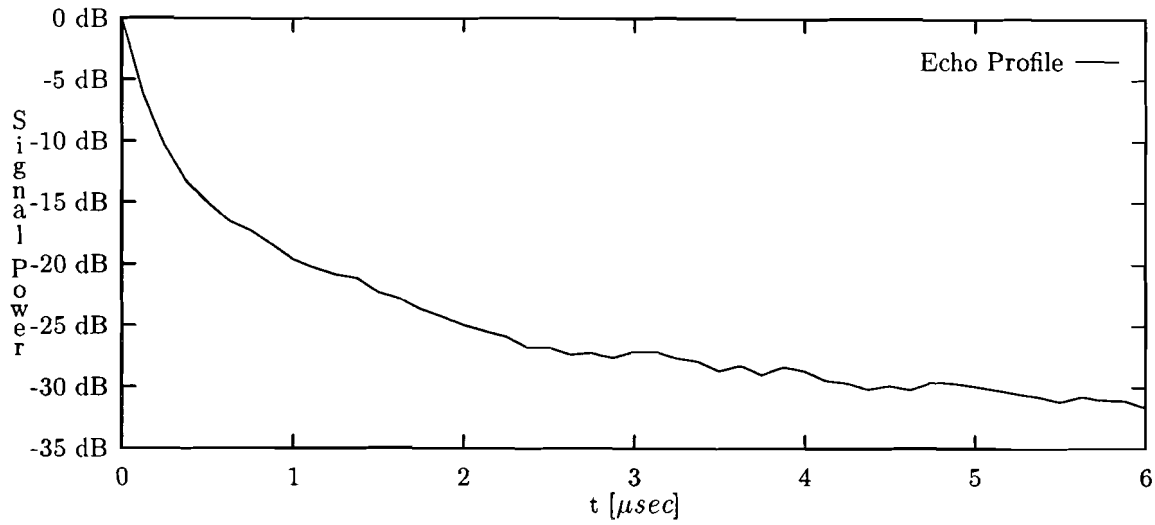

Figure 2.3: Averaged urban multipath intensity profile

If on a perfect channel, the power of a wide-band signal is uniformly distributed (at the transmitter side) over the available bandwidth, the received wide-band signal will also be uniformly distributed. The multipath channel however is not a perfect channel. Due to the delayed components of the transmitted signals that are received, the distribution of the power over the bandwidth at receiver side will not be uniform, but shows a more or less random power-distribution at the receiver. This effect is called frequency selectivity. The delay power spectrum is a description of the channel in the time domain. If we perform a Fourier Transform on the delay power spectrum, the transform relationship is simply

$$\phi_C(f) = \int_{-\infty}^{\infty} \phi_c(\tau) e^{-j2\pi f\tau} d\tau. \tag{2.11}$$

Since $\phi_C(f)$ is the power distribution in the frequency domain, it provides us with a measure of the frequency coherence of the channel. The *coherence bandwidth* B_c is the minimum frequency spacing over which the channel transfer function is essentially uncorrelated [22]. As a result of the Fourier transform relationship between $\phi_C(f)$ and $\phi_c(\tau)$, the coherence bandwidth becomes [22],

$$B_c = \frac{1}{T_m}. \tag{2.12}$$

If B_c is small in comparison to the bandwidth of the transmitted signal, the channel is said to be *frequency-selective*. On the other hand, if B_c is large in comparison to the bandwidth of the transmitted signal the channel is said to be *frequency-non-selective*, or *flat*.

Figure 2.4 shows an example of the received power spectrum of a signal with an originally flat spectrum, that was transmitted over a terrestrial channel (in an urban area). It can be seen that the received spectrum suffers from frequency selectivity. When we look at the coherence bandwidth of rural and urban environments, B_c is usually in the order of

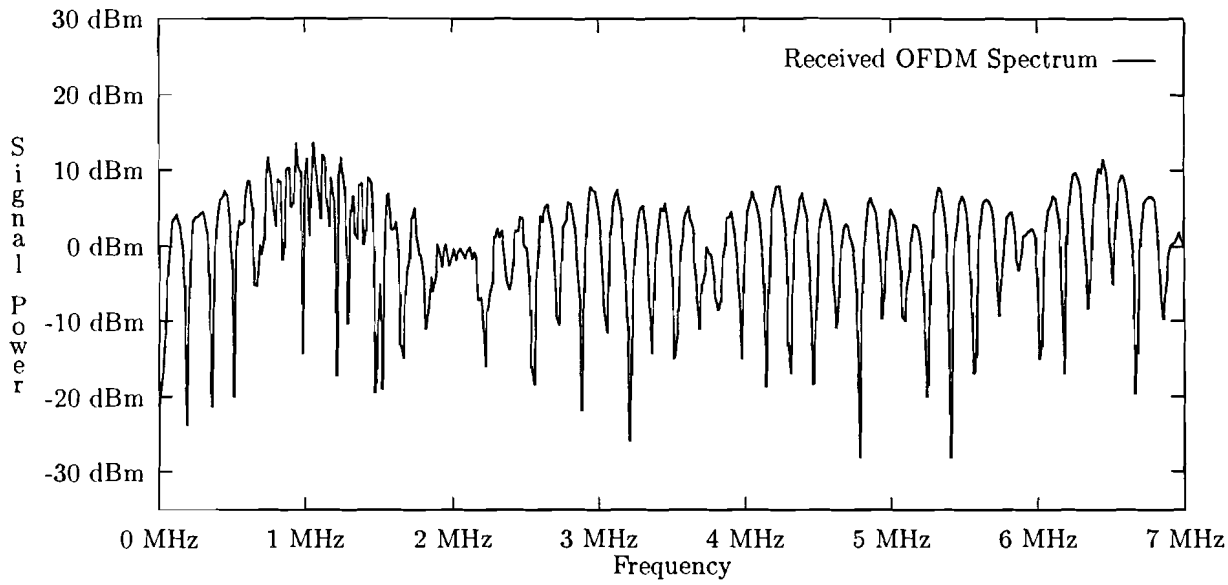

Figure 2.4: Received OFDM spectrum on a frequency selective channel

respectively 1.5 MHz and 150 kHz. In the urban environment, significant power variations take place within smaller bandwidths then in rural environments.

2.2.4 Characteristics of the multipath channel in the space domain

The multipath characteristics have already been described in the time and frequency domain. We assumed the receiving antenna to be at a fixed position. From measurements, it appears that the received narrow-band signal strength is very location dependent [7]. This effect is called spatial selectivity and is caused by local extinction of the signal contributions from the different paths in a multipath channel. The distance over which we need to shift the antenna in order to obtain uncorrelated reception conditions, is called the coherence distance X_c. Normally, the coherence distance is in the order of $\lambda/2$, where λ is the wavelength of the signal [15].

2.3 Orthogonal Frequency Division Multiplexing

This section describes the principles of Orthogonal Frequency Division Multiplexing (OFDM) [24]. OFDM forms the basis of proposed European digital broadcasting systems, where it is combined with frequency interleaving, coding and guard intervals [2].

2.3.1 Introduction to OFDM

The traditional way to transmit digital information over a channel, is to use single carrier modulation. If we use such a single carrier modulation system on a multipath channel,

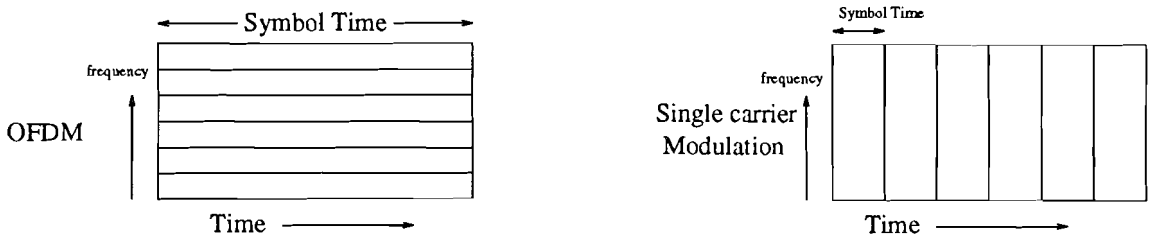

Figure 2.5: OFDM technique versus Single Carrier system.

we have to combat a major problem, called Inter Symbol Interference (ISI), introduced by signals from paths that arrive later in time (echoes). A very useful way to combat this problem is to add a guard interval to each information symbol. In this guard interval the information symbol is being extended cyclically. The loss in symbol rate can be kept small if ($T_s \gg T_g$), where T_s is the symbol time and T_g is the duration of the guard interval. The received signal will not suffer from ISI if $T_g \geq T_m$.

Example 1 *Let us consider a single carrier modulation system with a bandwidth of 10 Mhz. According to the Nyquist criterion [22], we should be able to reach a symbol rate of 10 Msymbol/s. The symbol time is 0.1 μs. When this signal is transmitted over an urban terrestrial channel, we will suffer from ISI. In section 2.2.2 we saw typical delay spread values of $T_m = 7\ \mu s$ for urban areas. The ISI can be eliminated by adding a guard interval to each transmitted symbol. For an urban environment, a guard interval of $T_g = 7\mu s$ should be sufficient. It can very easily be seen that we have developed a very inefficient system, because our net bit rate decreases enormously ($T_s \ll T_g$). One way to combat ISI and to reach a high spectral efficiency is to increase the symbol time. An increase of the symbol time means a decrease in required bandwidth. This is where the OFDM technique is very useful.*

OFDM is a technique for efficiently combining many narrow-band signals, using the Inverse Discrete Fourier Transform (IDFT), into a wide-band channel. At the receiver side, we use a Discrete Fourier Transform (DFT) to demultiplex the different subchannels. In section 2.3.2 the OFDM technique is described. In Section 2.3.3 is described how the guard intervals are used to prevent ISI.

2.3.2 The OFDM technique

In this section it is assumed that no guard intervals will be employed, i.e. $T_g = 0$. The OFDM technique permits the time-frequency domain to be split into small cells with dimensions of T_s and $f_s = \frac{1}{T_s}$ on the time and frequency axes respectively [24]. In Figure 2.5 OFDM and single carrier modulation are illustrated. It is clear that given a certain usable bandwidth, the net bit rate will be the same for both the OFDM and the single carrier technique. OFDM benefits from the fact that the symbol time is much larger.

Let $\{f_k\}$ be a set of N carrier frequencies such that

$$f_k = f_0 + \frac{k}{T_s} \qquad k = 0, 1, \cdots, N-1 \quad , \tag{2.13}$$

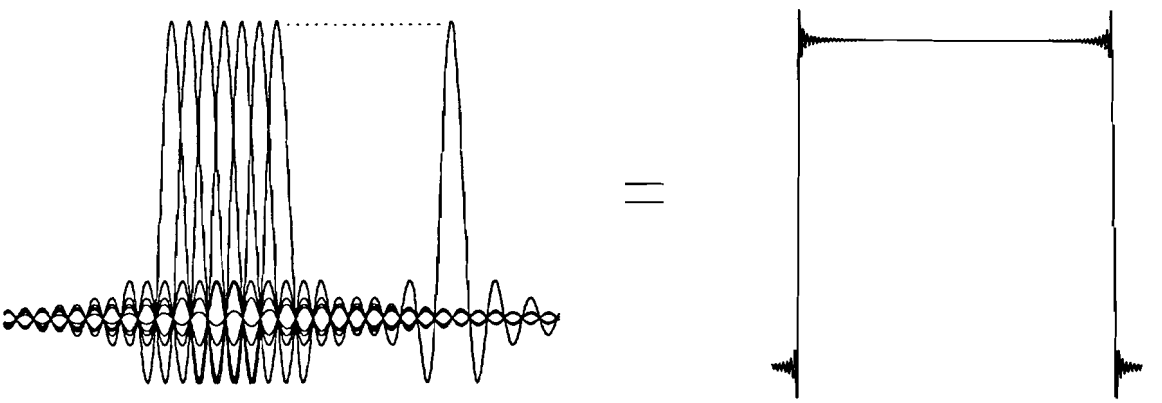

Figure 2.6: The OFDM signal

where T_s represents the time duration of the symbol. An orthogonal base of N signals is then defined as

$$\psi_{i,k}(t) = g_k(t - iT_s) \qquad k = 0, 1, \cdots, N-1 \quad , \quad -\infty < i < +\infty \tag{2.14}$$

where

$$g_k(t) = \begin{cases} e^{j2\pi f_k t} & 0 \leq t < T_s \\ 0 & \text{elsewhere} \end{cases} . \tag{2.15}$$

We can write $g_k(t) = x_k(t) \cdot y_k(t)$ such that

$$x_k(t) = e^{j2\pi f_k t} \qquad -\infty < t < \infty \tag{2.16}$$

and

$$y_k(t) = \begin{cases} 1 & 0 \leq t < T_s \\ 0 & \text{elsewhere} \end{cases} . \tag{2.17}$$

Now we can use one of the Fourier transform theorems (frequency translation) to calculate the Fourier transform $G_k(f)$ of $g_k(t)$. If we use this theorem on our signal $g_k(t)$, the Fourier transform is easily calculated.

$$G_k(f) = T_s \frac{\sin \pi(f - f_k)T_s}{\pi(f - f_k)T_s} \tag{2.18}$$

The signal spectra $G_k(f)$ mutually overlap as illustrated in Figure 2.6. The sum of all these overlapping elementary carriers leads to an almost flat rectangular power spectral density if there is an equal power division over the subchannels. The modulated OFDM signal can than be written as

$$s(t) = \sum_{i=-\infty}^{\infty} \sum_{k=0}^{N-1} s_{i,k} \psi_{i,k}(t), \tag{2.19}$$

where the complex symbol $s_{i,k}$ represents the amplitude-phase modulation applied to the $\psi_{n,k}$ signal. The received signal will suffer from signal fading and Additive White Gaussian Noise, i.e.,

$$r(t) = \alpha(t, f, x)\, s(t) + n(t), \tag{2.20}$$

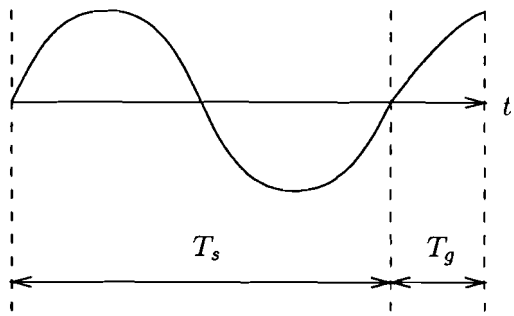

Figure 2.7: Symbol with guard interval.

where $\alpha(t, f, x)$ is the complex attenuation factor as a function of time, frequency and location and $n(t)$ is complex Gaussian noise with spectral density N_0. The demodulation method may then be expressed as

$$\hat{s}_{i,k} = \frac{1}{T_s} \int_{-\infty}^{\infty} r(t) \psi_{i,k}^*(t) dt \tag{2.21}$$

The sampled representation of the $r(t)$ signal in the time interval $[iT_s, (i+1)T_s]$ is given by the Inverse Discrete Fourier Transform (IDFT) of the complex coefficients $s_{i,k}$ with $k = 0, \ldots, N-1$. In practice, the modulation and demodulation processes are performed by means of Fast Fourier Transform algorithms.

2.3.3 The guard interval

Following the Nyquist criterion, a signal waveform (called a symbol) with a bandwidth f_s can be transmitted during a period T_s, where $f_s T_s = 1$. To overcome the problem of multipath echoes, which introduce ISI, we extend each symbol in time with a guard interval T_g, in which we cyclically repeat the first part of the symbol. Figure 2.7 illustrates this. Of course the guard interval should be at least as long as the multipath spread ($T_g \geq T_m$). At the receiver the extended symbol is observed in a window with the duration of the original symbol time T_s, in order to recover the transmitted symbol. This is indicated in Figure 2.8. The window is chosen in such a way that no ISI will occur within the window (Normally this window will be put at the end of the symbol). We have to be aware of the fact that shifting the window, corresponds with rotating the received symbol $\hat{s}$ in the complex plane. When the information is differentially encoded [22], we can still receive the symbols correctly, if the window is shifted not too rapidly in the time domain. If no differential encoding is applied, the channel state needs to be estimated.

2.4 OFDM parameters for a suggested transmission system

In [9], an example of a multi-resolution OFDM scheme is presented. The parameters from this scheme are used in this section.
It is proposed to use a scheme with a total bandwidth of $B = 8$ MHz. Because the

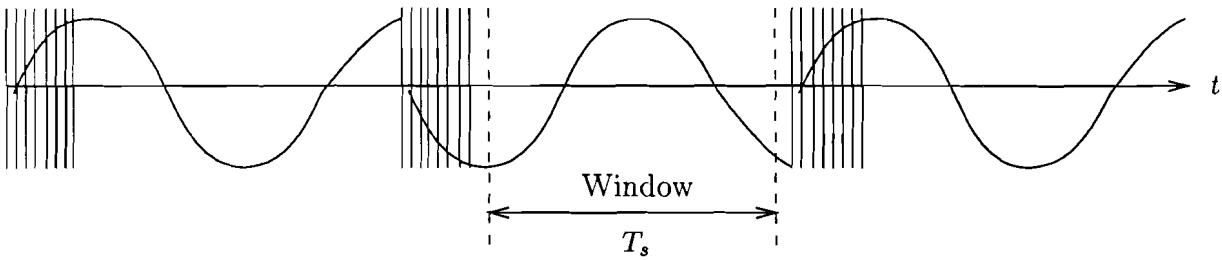

Figure 2.8: Received signal with multipath distortion. The shaded parts of the signal are disturbed with ISI.

transmission channel suffers from multi-path effects, a guard interval is added at the end of each symbol. A guard interval of $14\mu s$ is chosen to combat the multipath effects for an urban and rural terrain. In order to spend not more than 10% of the channel capacity to the guard interval, the symbol time is chosen to be $T_s = 128\mu s \approx 9T_g$. Now it is possible to transmit $1/(T_s + T_g) = 7042$ symbols/s over each OFDM channel, where every channel occupies a bandwidth of $f_s = 1/T_s = 7812.5$ Hz. It was already mentioned that a total bandwidth of 8 MHz is used. Using the OFDM technique,

$$N = \frac{B}{f_s} = 1024 \tag{2.22}$$

channels can be placed in a bandwidth of 8 MHz. Since we need guard bands for filtering, not more than 925 OFDM channels are used. The remaining 99 channels are modulated with a zero signal at both extremes of the 8 MHz spectrum. This reduces the total effective (used) bandwidth to 7.33 MHz. The total channel symbol rate becomes now $7042 \times 925 \approx 6.5$ Msymbol/s.

2.5 2-Resolution Transmission

Multi resolution signal constellations were first suggested by Cover in 1972 [11]. In the proposed system, 2-Resolution QAM is used. The signal constellation consists of 4 clouds with 4 signal points each. Such a constellation is referred to as 2R(2,2)-QAM. Figure 2.5 shows a 2R(2,2)-QAM signal constellation. The parameter $c = (d_b/d_g)^2$ determines the signal-to-noise ratio gain of the High Priority (HP) bits towards the Low Priority (LP) bits. The 2-resolution modulation technique is very useful in a situation where we want to provide services to fixed (rooftop antennas) receivers as well as portable receivers. Because portable receivers suffer much more from the multipath distortion than fixed receivers with a rooftop antenna, we can not efficiently provide the same service for both receivers. The system is developed to provide the 2 HP bits to portable receivers, fixed receivers should also be able to distinguish between the 4 LP points giving an extra 2 bits. If we consider 2R(2,2)-QAM to be a subset of the 64-QAM constellation, a gap of $c = 25$ (14 dB) seems still reasonable. This 2-resolution constellation implies that we can provide a gross bitrate of approximately 4×6.5 Msymbols/s=26 Mbit/s to a fixed receiver. A portable receiver on the other hand can receive a gross bit rate of 13 Mbit/s. From the source coding point of view we know that a bit rate of 5Mbit/s is sufficient to provide Standard Definition

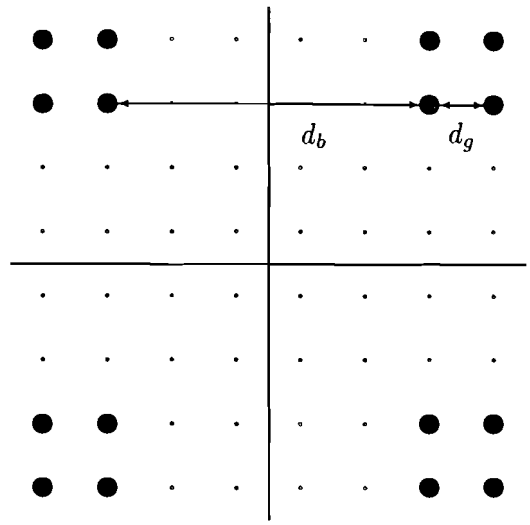

Figure 2.9: 2R(2,2)-QAM Signal Constellation

(SD) picture quality. We now can provide two SD quality programs to a portable receiver. If we use an additional 5Mbit/s for each program we can provide Enhanced Definition (ED) picture quality. A fixed receiver with a rooftop antenna should be able two receive two ED programs. It is also possible to provide a fixed receiver with 4 SD programs.

All bits transmitted are differentially encoded. The advantage of differential encoding is that we resolve the 90^o phase ambiguity problem, and that no phase recovery is necessary.

Throughout the rest of the report QPSK modulation will be used.

2.6 Error-Correcting coding

Error-correcting codes must provide sufficient protection to the LP and HP data in order to enable correct source decoding at the receiver. A remaining bit error rate, after decoding, of 10^{-10} is thought to be acceptable. The bit sequence produced at the information source is encoded with a $[n, n-2t, 2t+1]$ Reed-Solomon (RS) code where n is the code length, $n-2t$ is the number of information bytes and $2t+1$ is the minimum Hamming distance of the code [18]. Such a code is capable of correcting t random byte errors and has code-rate $R = \frac{n-2t}{n}$.

The HP bits are protected by a frequency interleaved RS[154,122,33] (code-rate $R = 0.79$). In each OFDM channel, the HP bits of 4 consecutive time slots are taken together and stored in one RS byte. Having 925 OFDM channels, we can store 6 RS[154,122,33] code words in 4 time slots with depth 6 frequency interleaving. For the LP-bits a same kind of code is proposed.

Table 2.1 shows an overview of the parameters that are defined in [9].

Table 2.1: Example of the proposed OFDM parameters

channel bandwidth	B	: 8 MHz (VHF is discarded)
effective bandwidth	B_{eff}	: 7.33 MHz (925 OFDM channels are used)
guard interval	T_g	: 14 μs
efficiency loss due to T_g		: 10 %
Modulation		: multi- resolution 16-QAM
$\Rightarrow$ FFT-size	N	: 1024
$\Rightarrow$ subcarrier spacing		: 7.8125 kHz
$\Rightarrow$ symbol time	$T_s + T_g$	: 142 μs
$\Rightarrow$ useful symbol time	T_s	: 128 μs
$\Rightarrow$ active subcarriers	N_{eff}	: 925
$\Rightarrow$ Channel bit rate (16-QAM)		: $925 \cdot 7042 \cdot 4 = 26.1$ Mbps
coding rate for portable reception	R_p	: 0.79
coding rate for fixed reception	R_f	: 0.79
net bit rate for portable receiver		: 10.3 Mbps
net bit rate for fixed receiver		: 20.6 Mbps
bit rate reserved for audio		: 512 kbps
bit rate reserved for data		: 128 kbps
bit rate reserved for SD picture quality		: 4.53 Mbps
bit rate reserved for ED picture quality		: 9.16 Mbps

Chapter 3

Antenna Diversity, theory

3.1 Introduction

Antenna diversity can be obtained by using more than one antenna at the receiver side. Antenna diversity is often used for improving the reception quality of a transmitted signal. Different antenna diversity techniques like space diversity, polarization diversity and angle diversity are described in Section 3.3. Antenna diversity will probably have the greatest effect at locations where reception conditions are poor. Portable and mobile reception fall into this category.

The signals received with the different antennas, when a certain diversity technique is applied, need to be combined in a combiner. Some combining techniques such as maximum ratio combining, equal gain combining and selection combining are described in Section 3.4. In Section 3.5 is described how the combining can be carried out for OFDM systems.

3.2 The History of Antenna Diversity

In most literature about antenna diversity, the first reference are two articles written by Beverage and Peterson [5, 20]. Beverage and Peterson carried out research on antenna diversity and built a diversity combiner in 1931. The diversity combiner described in their article consists of three spaced antennas that are connected to three receivers. The output of each receiver is rectified and the d-c outputs are combined with a common resistor. This combining technique could nowadays best be described by equal gain combining (section 3.4.2).

A few years before Beverage and Peterson started their work on antenna diversity, A. de Haas already had carried out some work on antenna diversity in the Dutch East Indies [12, 13]. His diversity system was used for telegraphy communication. The articles he wrote about antenna diversity were published in a Dutch magazine called "Radio-Nieuws". De Haas describes in his articles a very primitive form of antenna diversity. He uses four antennas and four receivers. The outputs of the four receivers are combined. De Haas

writes that the average output power of each of the four receivers needs to be adjusted manually.

In 1959, Brennan wrote his famous article "Linear Diversity Combining Techniques" [10]. This article describes in an analytic way, different combining techniques. Articles and books about antenna diversity that where written after Brennan's article are in most cases based on this article.

Nowadays, antenna diversity has found many implementations. In [17], a diversity system for a driving car is described (developed by Philips [3, 4]). One of four antennas can be selected according to a certain selection criterion. The improvement of the received signal is large. Philips has also developed a car vision diversity system, where two antennas are used to improve the picture quality [21]. The car vision diversity system is developed in such a way that the antenna signal with the strongest sound carrier power is selected. Also cordless telephone systems can benefit from antenna diversity [19].

3.3 Antenna Diversity Techniques

The different antenna diversity techniques discussed here require that a number of antennas are available, each receiving the same signals information under independent fading statistics. Proper combining of the signals yields an improved detection reliability. In the following a number of different diversity techniques are described briefly.

3.3.1 Space Diversity

Consider an array of L antennas, where two following antennas in the array are spaced a distance x. This antenna diversity technique is called space diversity. This technique has found many applications over the years and is in wide use in a variety of present-day communication systems. It is relatively simple to implement. The basic requirement is that the spacing of the antennas is chosen such that the individual channel characteristics at the antennas are uncorrelated. In practice, spacings of $\lambda/2$ should be sufficient for obtaining sufficient uncorrelation [15]. The required spacing, depends heavily on the disposition of the scatterers causing the multipath transmission. Each of the L antennas in the diversity array provides an independent signal to an L-branch diversity combiner.

3.3.2 Polarization Diversity

In [15], it is shown that signals received with antennas that transmit/receive orthogonal polarizations exhibit uncorrelated fading characteristics. These signals thus can be used in diversity systems. If we use one vertically and one horizontally polarized antenna, the antenna configuration size may be minimum.

3.3.3 Angle Diversity

Angle diversity uses antennas with high directivity. The antennas can "look" at a certain direction. In the multipath channel scatterers may come from all directions. If we point these antennas at directions were strong scatterers are coming from a considerable gain can be achieved.

3.4 Combining techniques

We have described some ways of employing antenna diversity. In the following only space diversity is taken into account. The signals received with different diversity techniques have to be combined with a combiner. We want to design a combiner that maximizes the average signal-to-noise ratio $\overline{\gamma}$ and improves the resulting distribution of the signal-to-noise ratio γ. On each antenna j, $j = 1, \ldots, L$, we receive the narrow-band signal $r_j = \alpha_j s + n_j$. Throughout the rest of this chapter we assume $E^{(t)}[ss^*] = E_s$, $E^{(t)}[n_j n_j^*] = E^{(x)}[n_j n_j^*] = N_0$ and α_j is the complex attenuation factor of the j^{th} antenna signal[1] . We assume α_j to be mutually independent complex Gaussian distributed with $E^{(x)}[\alpha_j \alpha_j^*] = 1$. Thus α_j is assumed to be constant in time and only dependent on the antenna location. The average signal-to-noise ratio $\overline{\gamma}_j$ at antenna j becomes

$$\overline{\gamma}_j = E^{(x)}\left[\frac{E^{(t)}[(\alpha_j s)(\alpha_j s)^*]}{E^{(t)}[n_j n_j^*]}\right] = \frac{E_s}{N_0}. \tag{3.1}$$

A combiner generates a combined signal

$$r_c = \sum_{j=1}^{L} \beta_j r_j, \tag{3.2}$$

where β_j is the weighting factor of antenna j. The most well-known combining techniques are described below, where the assumption is made that the $|\alpha_j|$ values are Rayleigh distributed.

3.4.1 Maximum Ratio Combining

In this method, the L signals are added up, each weighted with the complex conjugate α_j^* of α_j (hence, $\beta_j = \alpha_j^*$). This means that the individual signals are cophased before addition. Maximum ratio combining is proved to be the optimal linear combining technique [10]. Assuming that the channel state can be estimated perfectly we get

$$r_{mr} = \sum_{j=1}^{L} \alpha_j^* r_j = s \sum_{j=1}^{L} \alpha_j^* \alpha_j + \sum_{j=1}^{L} \alpha_j^* n_j. \tag{3.3}$$

The resulting signal-to-noise ratio γ_{mr} becomes

$$\gamma_{mr} = \frac{E^{(t)}\left[\left|s \sum_{j=1}^{L} \alpha_j \alpha_j^*\right|^2\right]}{E^{(t)}\left[\left|\sum_{j=1}^{L} \alpha_j^* n_j\right|^2\right]} = \frac{E_s}{L N_0}\left(\sum_{j=1}^{L} \alpha_j \alpha_j^*\right)^2 \tag{3.4}$$

[1] $E^{(t)}[\xi]$ represents the time average and $E^{(x)}[\xi]$ represents the location average.

and the average signal-to-noise ratio at the output of the maximum ratio combiner becomes

$$\overline{\gamma}_{mr} = E^{(x)}[\gamma_{mr}] = E^{(x)}\left[\left(\frac{E_s}{LN_0}\sum_{j=1}^{L}\alpha_j\alpha_j^*\right)^2\right] = \frac{E_s}{LN_0}L^2 = \frac{LE_s}{N_0} = L\overline{\gamma}_j. \qquad (3.5)$$

Thus, antenna diversity with maximum ratio combining improves the average signal-to-noise ratio with a factor L.

In order to employ an explicit distribution of the signal-to-noise ratio γ, we will, without loss of generality, employ for the received signal $r_j = \alpha_j s + n_j$ the following assumptions: $E[n_j n_j^*] = 1$ and $E[ss^*] = 1$. The local signal-to-noise ratio γ_j becomes $\gamma_j = |\alpha_j|^2$. It will be assumed that the variables $|\alpha_j|$ follow a Rayleigh distribution with density function

$$p_{|\alpha_j|}(a) = \begin{cases} 2ae^{-a^2} & (a \geq 0) \\ 0 & (a < 0) \end{cases} \qquad (3.6)$$

and distribution function

$$P[\alpha_j \leq a] = \begin{cases} 1 - e^{-a^2} & (a \geq 0) \\ 0 & (a < 0) \end{cases} \qquad (3.7)$$

Writing the Rayleigh distribution in the form of (3.6) and (3.7) implies a particular choise of scale; in particular $E[\alpha_j\alpha_j^*] = 1$. With (3.7) and the fact that $\gamma_j = |\alpha_j|^2$ we can calculate the distribution function for γ_j.

$$P[\gamma_j \leq \gamma] = \begin{cases} 1 - e^{-\gamma} & (\gamma \geq 0) \\ 0 & (\gamma < 0) \end{cases} \qquad (3.8)$$

The density function $p_{\gamma_j}(\gamma)$ becomes now

$$p_{\gamma_j}(\gamma) = \begin{cases} e^{-\gamma} & (\gamma \geq 0) \\ 0 & (\gamma < 0) \end{cases} \qquad (3.9)$$

Equations (3.8) and (3.7) are distribution functions of the situation where one single antenna is used and therefore no combining is applied. We are interested in the distribution of the sum $\gamma_{mr} = \sum \gamma_j$ of L independent random variables each with distribution (3.8). We know that $\gamma_j = (x_j^2 + y_j^2)$, where x_j and y_j are independent Gaussian variables of equal variance $\frac{1}{2}$ and zero mean. Thus γ_{mr} is a chi-square distribution of $2L$ random variables [15]. The probability density function of $\gamma_m r$ (when L antennas are used) can than be immediately written down as [10]

$$p_{\gamma_{mr}^{(L)}}(\gamma_j) = \frac{1}{(L-1)!}\gamma_j^{L-1}e^{-\gamma_j}. \qquad (3.10)$$

Integration of the density function gives the distribution function

$$P[\gamma_{mr}^{(L)} \leq \gamma_j] = \frac{1}{(L-1)!}\int_0^{\gamma_j} y^{L-1}e^{-y}dy. \qquad (3.11)$$

By using $P[\gamma_{mr}^{(1)} \leq \gamma_j] = 1 - e^{-\gamma_j}$ and the recursion relation $P[\gamma_{mr}^{(L)} \leq \gamma_j] = P[\gamma_{mr}^{(L-1)} \leq \gamma_j] - p_{\gamma_{mr}^{(L)}}(\gamma_j)$, we have,

$$P[\gamma_{mr}^{(2)} \leq \gamma_j] = 1 - (1 + \gamma_j)e^{-\gamma_j}, \qquad (3.12)$$

$$P[\gamma_{mr}^{(3)} \leq \gamma_j] = 1 - \left(1 + \gamma_j + \frac{\gamma_j^2}{2}\right) e^{-\gamma_j}, \tag{3.13}$$

and in general,

$$P[\gamma_{mr}^{(L)} \leq \gamma_j] = 1 - \left(\sum_{n=0}^{L-1} \frac{\gamma_j^n}{n!}\right) e^{-\gamma}. \tag{3.14}$$

This distribution function gives an indication about how much the signal can be improved using more than one antenna. Figure 3.1 and 3.2 graphically illustrate the density and distribution functions.

3.4.2 Equal gain combining

Equal gain combining also assumes we can make a perfect estimate of the phase of the different α_j values. The L signals are added up each corrected for their own phase, hence $\beta_j = \frac{\alpha_j^*}{|\alpha_j|}$. The combined signal becomes

$$r_{eg} = \sum_{j=1}^{L} \frac{\alpha_j^*}{|\alpha_j|} r_j = s \sum_{j=1}^{L} \frac{\alpha_j \alpha_j^*}{|\alpha_j|} + \sum_{j=1}^{L} \frac{\alpha_j^*}{|\alpha_j|} n_j = s \sum_{j=1}^{L} |\alpha_j| + \sum_{j=1}^{L} \frac{\alpha_j^*}{|\alpha_j|} n_j. \tag{3.15}$$

The resulting signal-to-noise ratio becomes

$$\gamma_{eg} = \frac{E^{(t)}\left[\left|s \sum_{j=1}^{L} |\alpha_j|\right|^2\right]}{E^{(t)}\left[\left|\sum_{j=1}^{L} n_j\right|^2\right]}. \tag{3.16}$$

With $E[ss^*] = E_s$ and $E[n_j n_j^*] = N_0$, (3.16) becomes

$$\gamma_{eg} = \frac{E_s}{N_0 L}\left(\sum_{j=1}^{L} |\alpha_j|\right)^2 = \frac{E_s}{N_0 L}\left(\sum_{j=1}^{L} |\alpha_j|^2 + \sum_{j=1}^{L} \sum_{k=1, k\neq j}^{L} |\alpha_j||\alpha_k|\right). \tag{3.17}$$

Since the assumption was made that the different α_j values are uncorrelated, $E[|\alpha_j||\alpha_k|] = E[|\alpha_j|]E[|\alpha_k|]$, if $j \neq k$. The average signal-to-noise ratio $\overline{\gamma}_{eg}$ becomes

$$\overline{\gamma}_{eg} = E^{(x)}[\gamma] = \frac{E_s}{LN_0}\left(L + \sum_{j=1}^{L} \sum_{k=1, k\neq j}^{L} E^{(x)}[|\alpha_i|]E^{(x)}[|\alpha_j|]\right). \tag{3.18}$$

If we assume that α_j is zero mean complex Gaussian distributed, the $|\alpha_j|$ values are Rayleigh distributed. For the Rayleigh distribution $E[|\alpha_j|] = \sqrt{\pi/2}$ (Appendix A). The average signal-to-noise ratio at the output of the combiner, when L antennas are used, becomes

$$\overline{\gamma}_{eg} = \frac{E_s}{N_0}\left(1 + (L-1)\frac{\pi}{4}\right). \tag{3.19}$$

From (3.19) we can see that $\overline{\gamma}_{eg}$ increases linearly with the number of antennas used. This was also the case for maximum ratio combining.

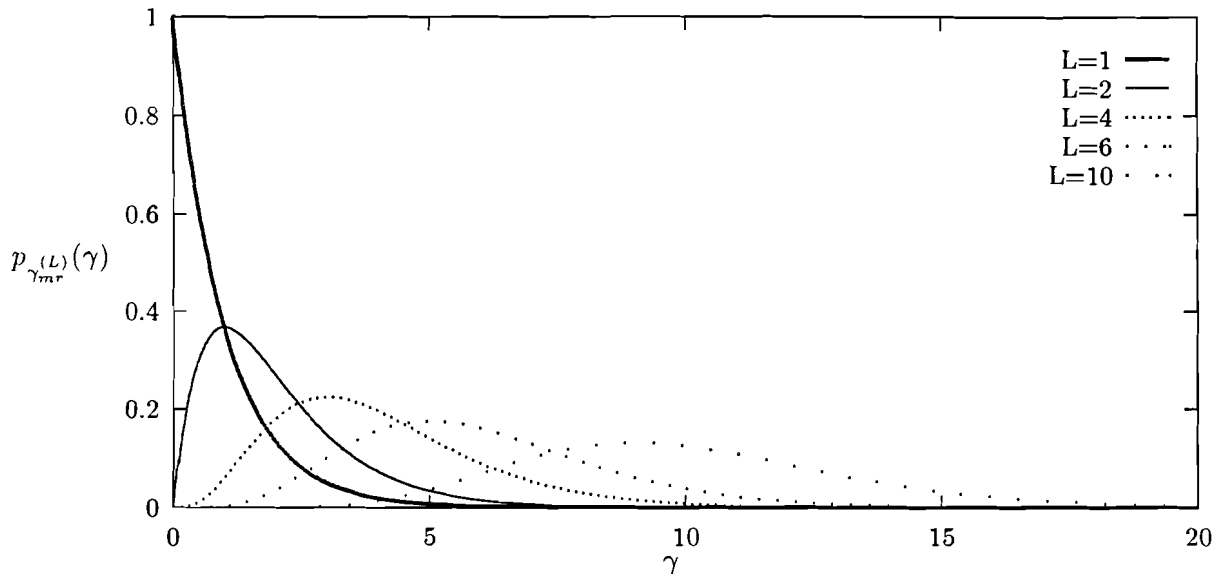

Figure 3.1: Probability density function of γ for L-branch maximum ratio combining when $E[n_j n_j^*] = 1$ and $E[ss^*] = 1$.

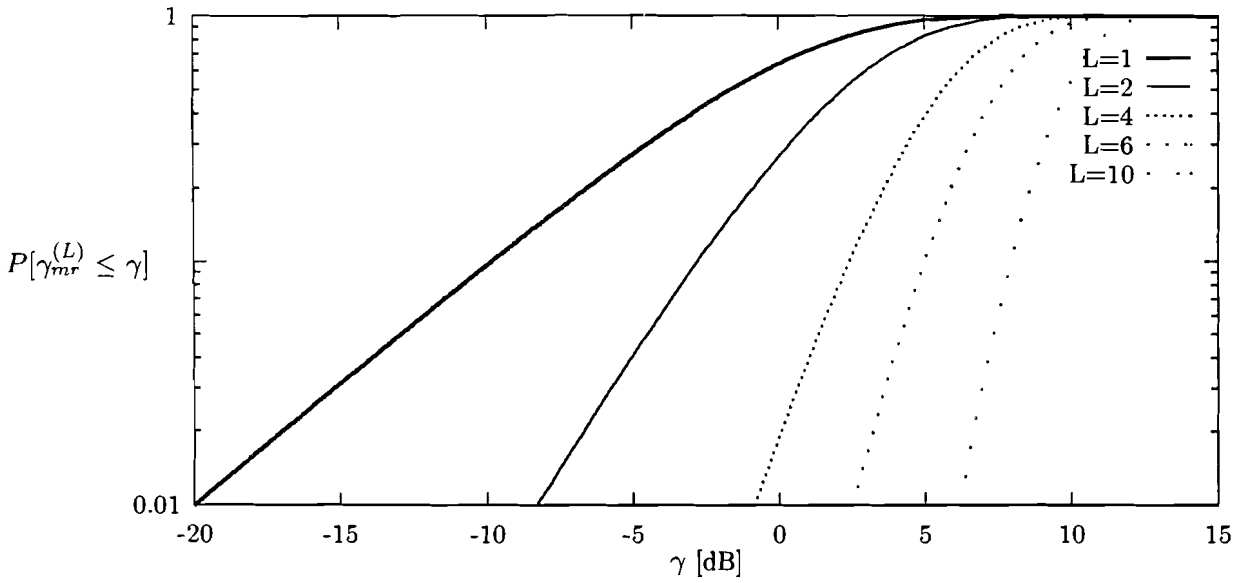

Figure 3.2: Probability distribution function of γ for L-branch maximum ratio combining when $E[n_j n_j^*] = 1$ and $E[ss^*] = 1$.

3.4.3 Selection Combining

This combining technique is a switching technique. The combining rule here is that, at any given time, the combiner simply picks out the best of L signals. More precisely, let k denote the index of a system where $\gamma_k \geq \gamma_j$, $j = 1, 2, \ldots, L$. Than this type of system is characterized by the design criterion

$$\beta_j = \begin{cases} 1 & (j = k) \\ 0 & (j \neq k) \end{cases} \tag{3.20}$$

The distribution function for an L-channel selection diversity system is particularly simple to obtain, provided the local noise powers $E^{(t)}[n_j n_j^*]$ are equal for all antennas. Again, assume $E[n_j n_j^*] = 1$ and that the $|\alpha_j|$ values are Rayleigh distributed. Then the individual signal-to-noise ratios γ_j have the distribution of (3.7). By (3.20), the output signal-to-noise ratio is the largest of the of the individual γ_j. If the largest $\gamma_j = x$, then the local signal-to-noise ratio of every channel $\gamma_j \leq x$. Hence, the output of the selection combiner will also have $\gamma_{sc} \leq x$. This means that the probability that the signal-to-noise ratio of the selection combiner $\gamma_{sc} \leq x$, is equal to the probability that all the L signal-to-noise ratios $\gamma_j \leq x$. Because the channel conditions at the different antennas are uncorrelated it is very easy to calculate the probability distribution function $P[\gamma_{sc}^{(L)} \leq \gamma_j]$ and the probability density function $p_{\gamma_{sc}^{(L)}}(\gamma_j)$ of a selection combiner.

$$\begin{aligned} P[\gamma_{sc}^{(L)} \leq \gamma_j] &= P[\gamma_1 \leq x, \ldots, \gamma_L \ldots x] \\ &= P[\gamma_1 \leq x] \cdot \ldots \cdot P[\gamma_L \leq x] = (P[\gamma_j \leq x])^L \\ &= (1 - e^{-\gamma})^L \end{aligned} \tag{3.21}$$

and

$$p_{\gamma_{sc}^{(L)}}(\gamma_j) = dP[\gamma_{sc}^{(L)} \leq \gamma_j] = L\,(1 - e^{-\gamma})^{L-1}\, e^{-\gamma} \tag{3.22}$$

Figure 3.3 and 3.4 graphically show the density and distribution functions for a different number of branches L. It is also interesting to known how the average signal-to-noise ratio $\overline{\gamma}_{sc}$ at the output of the combiner is improved. We know,

$$\overline{\gamma}_{sc} = \int_0^\infty \gamma p_{\gamma_{sc}^{(L)}}(\gamma_j) d\gamma = \int_0^\infty \gamma L\,(1 - e^{-\gamma})^{L-1}\, e^{-\gamma} d\gamma \tag{3.23}$$

We make the substitution of $y = 1 - e^{-\gamma}$ and $dy = e^{-\gamma} d\gamma$, and obtain

$$\overline{\gamma}_{sc} = L \int_0^1 [-\log(1 - y)]\, y^{L-1} dy. \tag{3.24}$$

Using the series [1]

$$-\log(1 - y) = \sum_{k=1}^{\infty} \frac{y^k}{k} \quad for\ |y| < 1, \tag{3.25}$$

$\overline{\gamma}_{sc}$ becomes,

$$\overline{\gamma}_{sc} = L \int_0^1 \left[\sum_{k=1}^{\infty} \frac{y^{k+L-1}}{k} \right] dy = L \sum_{k=1}^{\infty} \int_0^1 \frac{y^{k+L-1}}{k} dy$$

$$= \sum_{k=1}^{\infty} \frac{L}{k(k+L)} = \sum_{k=1}^{\infty} \left(\frac{1}{k} - \frac{1}{L+k} \right) = \sum_{k=1}^{\infty} \frac{1}{k} - \sum_{k=L+1}^{\infty} \frac{1}{k}$$

$$= \sum_{k=1}^{\infty} \frac{1}{k} - \left(\sum_{k=1}^{\infty} \frac{1}{k} - \sum_{k=1}^{L} \frac{1}{k} \right) = \sum_{k=1}^{L} \frac{1}{k}. \tag{3.26}$$

In general, when $E[ss^*] = E_s$ and $E[n_j n_j^*] = N_0$, (3.26) becomes

$$\overline{\gamma}_{sc} = \frac{E_s}{N_0} \sum_{k=1}^{L} \frac{1}{k}. \tag{3.27}$$

We can see that the $\overline{\gamma}_{sc}$ does not increase linearly with the number of antennas used. This in contrary of maximum-ratio and equal-gain combining. This is easily explained by the fact that on every instant only one antenna signal is processed. When a small number of antennas are used, selection combing can compete very well with equal gain and maximum ratio combining.

3.4.4 Power Ratio combining

Power Ratio combining is a combining technique that doesn't take into account the phase information of the received signals (a so called non-coherent combining technique). If we can make a perfect estimate of the envelope $|\alpha_j|$ of the received signals, we can combine the L signals by adding them up each multiplied with the envelope $|\alpha_j|$. The combined signal r becomes

$$r = \sum_{j=1}^{L} |\alpha_j| r_j = s \sum_{j=1}^{L} |\alpha_j| \alpha_j + \sum_{j=1}^{L} |\alpha_j| n_j \tag{3.28}$$

The signal-to-noise ratio γ_{pr} can be calculated and becomes

$$\gamma_{pr} = \frac{E^{(t)} \left[\left| s \sum_{j=1}^{L} |\alpha_j| \alpha_j \right|^2 \right]}{E^{(t)} \left[\left| \sum_{j=1}^{L} |\alpha_j| n_j \right|^2 \right]} = \frac{E_s \left| \sum_{j=1}^{L} |\alpha_j| \alpha_j \right|^2}{N_0 \sum_{j=1}^{L} |\alpha_j|^2} \tag{3.29}$$

If we make the substitution $\alpha_j = a_j e^{j\theta_j}$ where θ_j is the phase of the jth received signal and $a_j = |\alpha_j|$, γ_{pr} becomes

$$\gamma_{pr} = \frac{E_s \left(\sum_{j=1}^{L} a_j^4 + \sum_{j=1}^{L} \sum_{k=1, j \neq k}^{L} a_j^2 a_k^2 e^{j(\theta_j - \theta_k)} \right)}{N_0 \sum_{j=1}^{L} a_j^2}. \tag{3.30}$$

Because power ratio combining does not take the phase information into account, the improvement of the average signal-to-noise ratio is very poor. For this same reason the average signal-to-noise ratio $\overline{\gamma}_{pr}$ and the improvement of the distribution will not be examined.

3.4.5 Adding up L signals in a non-coherent manner

This section describes a combining technique that just adds up L received signals ($\beta_j = 1$ for all j). It will be shown that this combining technique does not improve the performance of a system. The received signal at the output of the combiner becomes

$$r_{nc} = \sum_{j=1}^{L} r_j = s \sum_{j=1}^{L} \alpha_j + \sum_{j=1}^{L} n_j. \tag{3.31}$$

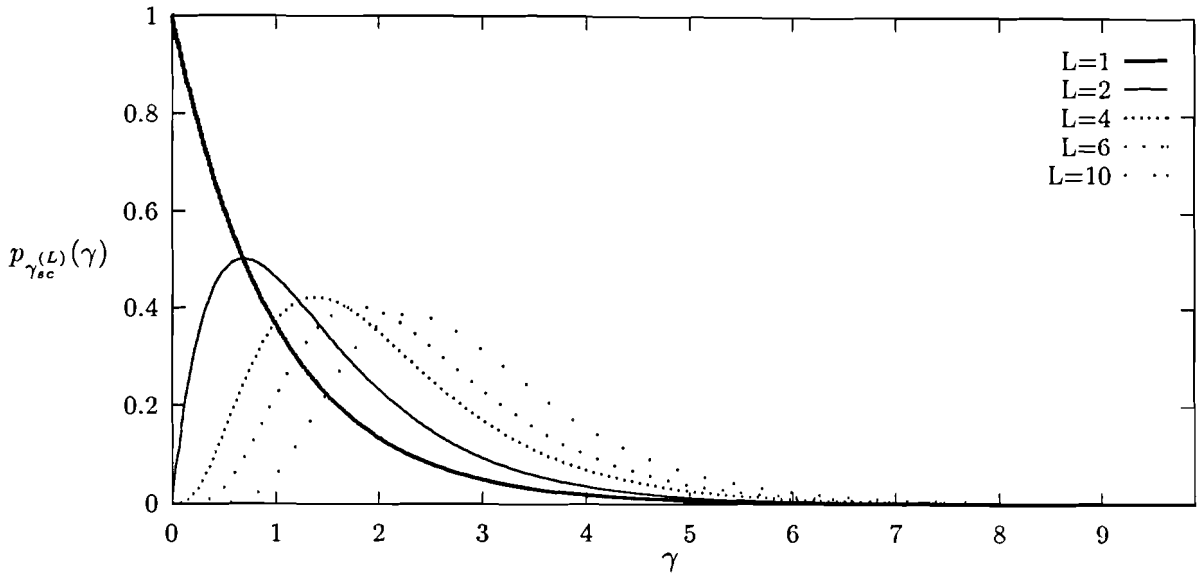

Figure 3.3: Probability density function of γ for L-branch selection combining when $E[n_j n_j^*] = 1$ and $E[ss^*] = 1$.

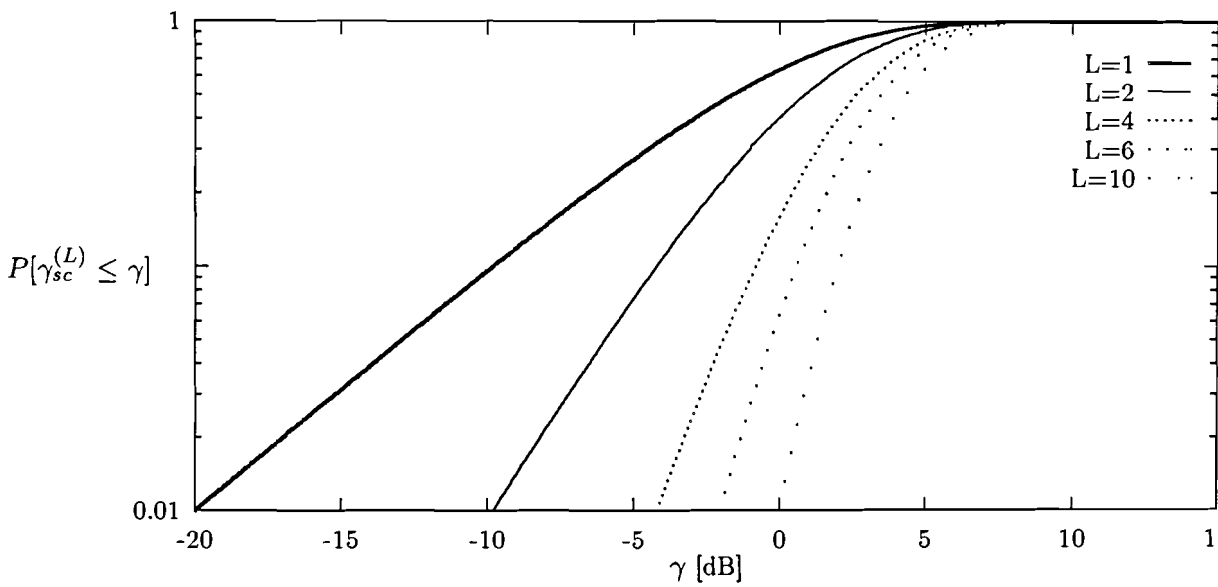

Figure 3.4: Probability distribution function of γ for L-branch selection combining when $E[n_j n_j^*] = 1$ and $E[ss^*] = 1$.

The resulting signal-to-noise ratio becomes

$$\gamma_{nc} = \frac{E^{(t)}\left[\left(s\sum_{j=1}^{L}\alpha_j\right)^2\right]}{E^{(t)}\left[\left(\sum_{j=1}^{L}n_j\right)^2\right]} = \frac{E_s}{LN_0}\left(\sum_{j=1}^{L}\alpha_j\right)^2 = \frac{E_s}{LN_0}\sum_{j=1}^{L}|\alpha_j|^2. \tag{3.32}$$

The substitution

$$\left(\sum_{j=1}^{L}\alpha_j\right)^2 = \sum_{j=1}^{L}|\alpha_j|^2$$

can be made because the α_j values are complex Gaussian distributed and mutually uncorrelated. The average signal-to-noise ratio at the output of the combiner becomes

$$\overline{\gamma}_{nc} = \frac{E_s}{LN_0}E^{(x)}\left[\sum_{j=1}^{L}|\alpha_j|^2\right] = \frac{E_s}{LN_0}\sum_{j=1}^{L}E^{(x)}\left[|\alpha_j|^2\right] = \frac{E_s}{N_0} = \overline{\gamma}_j. \tag{3.33}$$

We can see that the average signal-to-noise ratio at the output of the combiner equals the average signal-to-noise ratio of the system when no combining was applied. The performance of the system is not improved, actually a new antenna with other characteristics is generated.

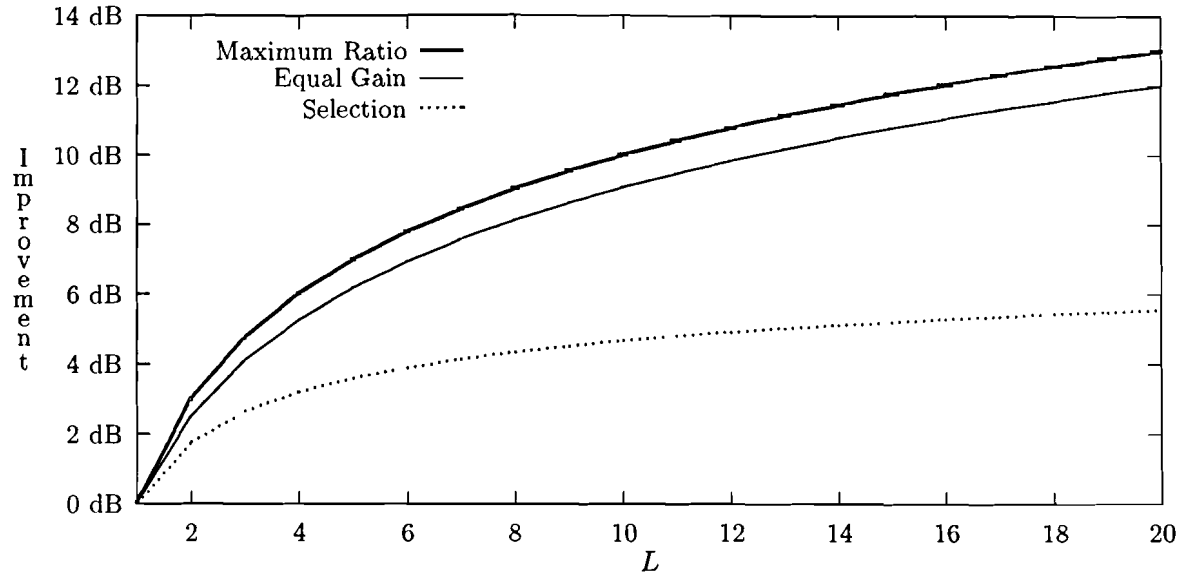

Figure 3.5: Improvement of average signal-to-noise ratio for different combining techniques

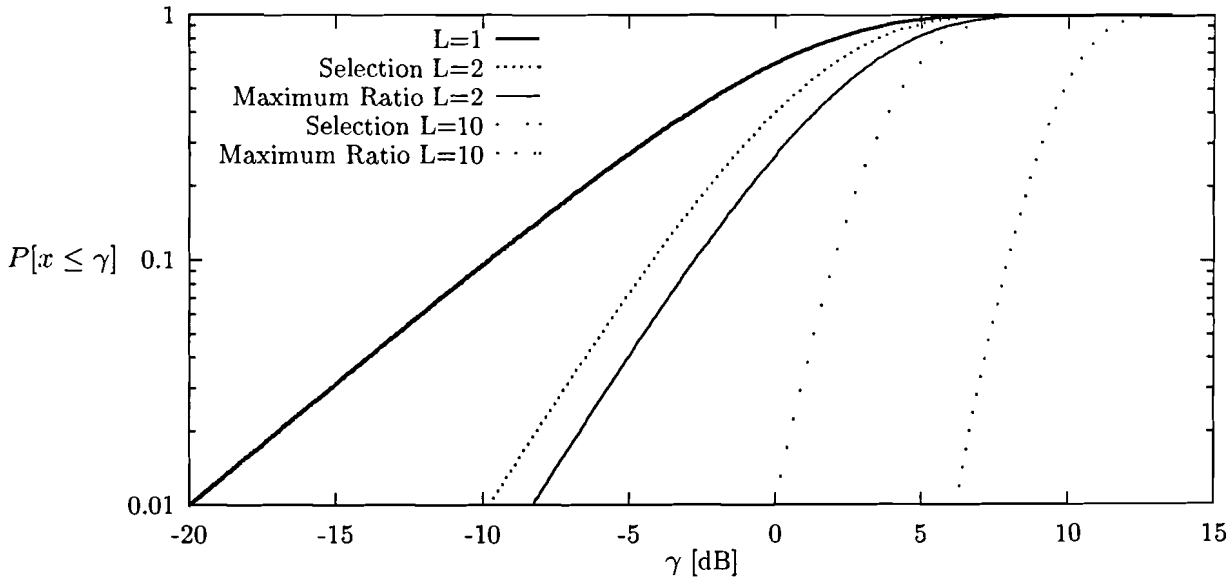

Figure 3.6: Difference in distribution of γ between Maximum Ratio and Selection combining when $E[n_j n_j^*] = 1$ and $E[ss^*] = 1$.

3.4.6 Comparison of the combining techniques

Several combining methods were examined. In this section the differences between the combining methods are discussed. It has been stated that combining methods taking into account the phase information of the received signals will perform much better than combining techniques that don't. Figure 3.5 shows the improvement of the average signal-to-noise ratio for different combining techniques as a function of the number of branches L. If we look at the situation where only $L = 2$ antennas are used, maximum ratio combining has an average signal-to-noise ratio of 0.5 and 1.3 dB larger then respectively equal gain and selection combining. Figure 3.6 shows the difference in the distribution of maximum ratio and selection combining. The more branches are used the better Maximum Ratio performs. In a diversity system where only two branches are used, selection combining is a good solution. In practical systems, a variant of selection combining, scanning diversity, is often used. Scanning diversity is a switching technique where you only choose another antenna if the signal of the current antenna drops below a certain threshold value.

There are many different methods to determine the system improvement when antenna diversity is applied. For example one can examine the fraction of time that the received signal is under a certain unacceptable value. It is a very useful way of determining the improvement of the system. The dTTb project in which Philips is active, is not yet in a state of development where one can determine a particular level where the received signal is acceptable. Thus it is not possible to define system improvement in terms of time that the received signal is under a threshold value. If we consider a RS-coded system, we can determine the signal-to-noise ratio $(\frac{S}{N})_1$ needed to reach a certain bit error rate. If we calculate the signal-to-noise ratio $(\frac{S}{N})_2$ again when antenna diversity is applied, we can define the system improvement to be,

$$G = \left(\frac{S}{N}\right)_1 - \left(\frac{S}{N}\right)_2 \tag{3.34}$$

where G is the gain which is, as well as the S/N values, expressed in dB. This method of determining the system improvement is used in this report.

In [6], the performance of $L = 2$ antenna diversity reception is analyzed on an infinitely interleaved Rayleigh fading channel. A RS[255,223,33] code was used. The bits were QPSK modulated. The performances are depicted in Figure 3.9. From Figure 3.9 we can derive that a significant performance improvement is achieved when maximum ratio, equal gain or selection combining are applied.

3.5 Antenna diversity for coded OFDM systems

Until now it was assumed that the transmitted signal s was a narrow band signal, i.e. $B_c \gg B$, where B is the bandwidth of the transmitted signal. This implies that the α_j values are constant over the bandwidth. The OFDM signal with B=8 MHz, on the other hand, is a wide-band signal with respect to the coherence bandwidth. In a broadcast situation with indoor portable reception, the coherence bandwidth can be very small. The α_j values will no longer be constant over the bandwidth of 8 MHz. Frequency selectivity

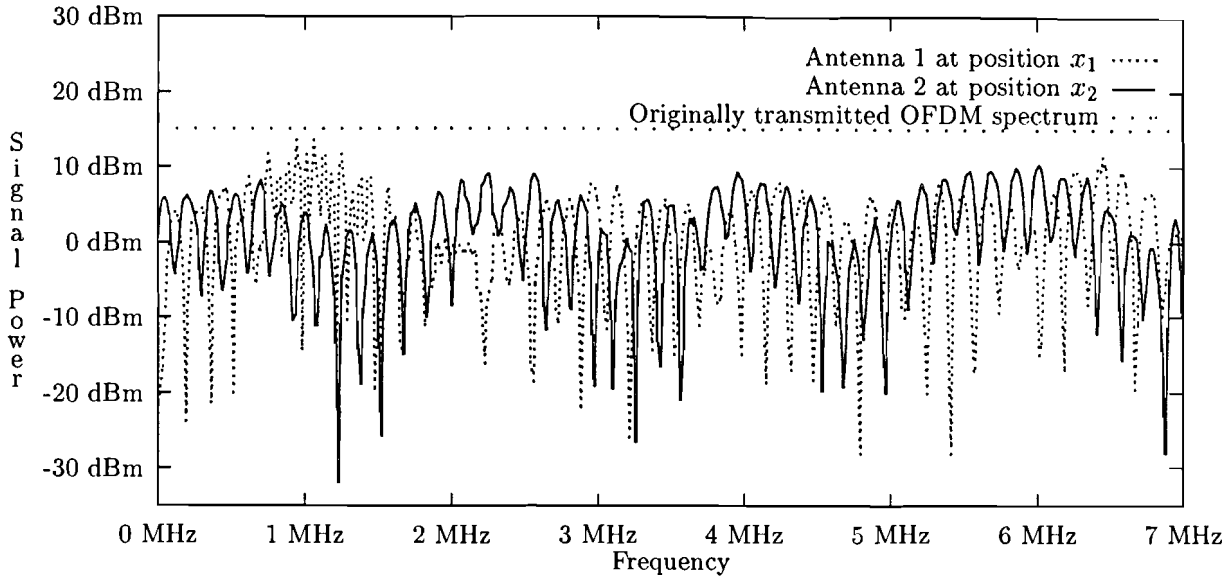

Figure 3.7: Received power spectrum at positions x_1 and x_2, $x_1 - x_2 = \lambda/2$.

is introduced. Figure 3.7 shows two received OFDM power spectra with two different antennas spaced by $\lambda/2$. The originally transmitted (flat) OFDM spectrum is also shown. Maximum ratio combining can not be realized for such wide-band signals, since it is not possible to define one complex attenuation factor α_j for the wide-band signal. Selection combining could be applied. The strongest signal could be selected and processed. Because the received suffers from both frequency selectivity and spatial selectivity and the fact that there is only a little variation in the total received wide-band power, wide-band selection combining will not result in much gain.

In [6], it is suggested to perform the combining for each subchannel separately. In other words, the front-end and OFD demultiplexer need to be implemented L fold. The outputs of the different OFD demultiplexers are fed to N combiners. N represents the number of subchannels in the OFDM signal and L denotes the number of antennas used. A diversity receiver of such a scheme is shown in Figure 3.8. Much higher gain can be achieved with this kind of narrow-band combining on a frequency selective fading channel. This type of narrow-band combiner has two benefits. First, it is possible to implement maximum ratio combining because we can define a complex attenuation factor $\alpha_{j,i}$ for each ith channel in the OFDM signal at the jth antenna. Secondly, we can perform the combining much more effectively because the combining can take place for each OFDM channel separately. The results of Figure 3.9 were obtained with simulations where an infinitely interleaved Rayleigh fading channel was assumed. If the channel is infinitely interleaved, the complex attenuation factors $\alpha_{j,i}$ are uncorrelated. The assumption that the received signals at different antennas are uncorrelated can be considered to be valid, but the attenuation factors of the different OFDM subchannels at a certain antenna will be correlated in most practical situations.

With the aid of measurements this correlation can be obtained. From these same measurements and simulations, the performance improvement can be calculated for a certain

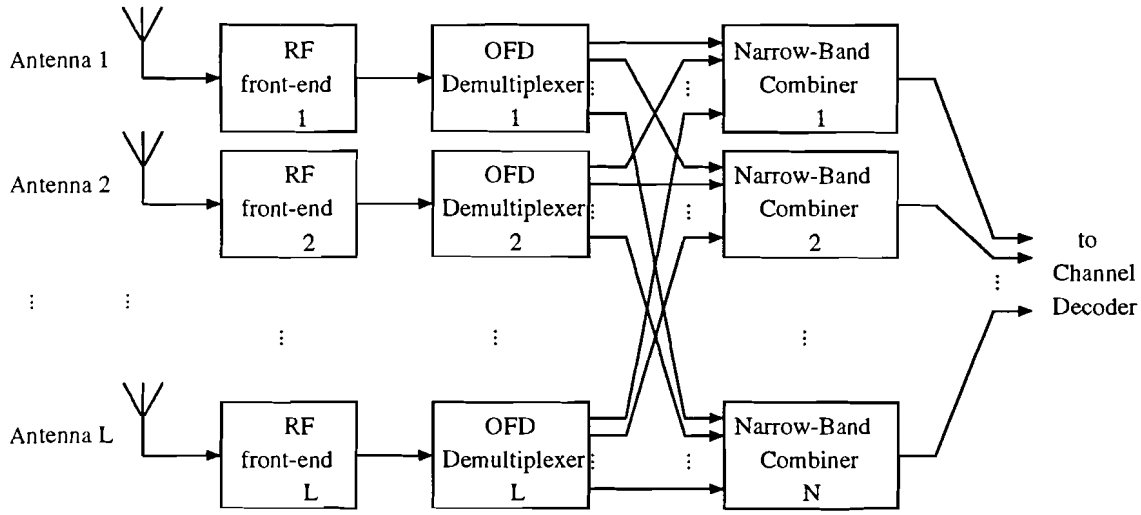

Figure 3.8: Narrow-Band combiner for an OFDM-based system; the front-end and OFD Demultiplexer are implemented L-fold; the combiner is implemented N-fold.

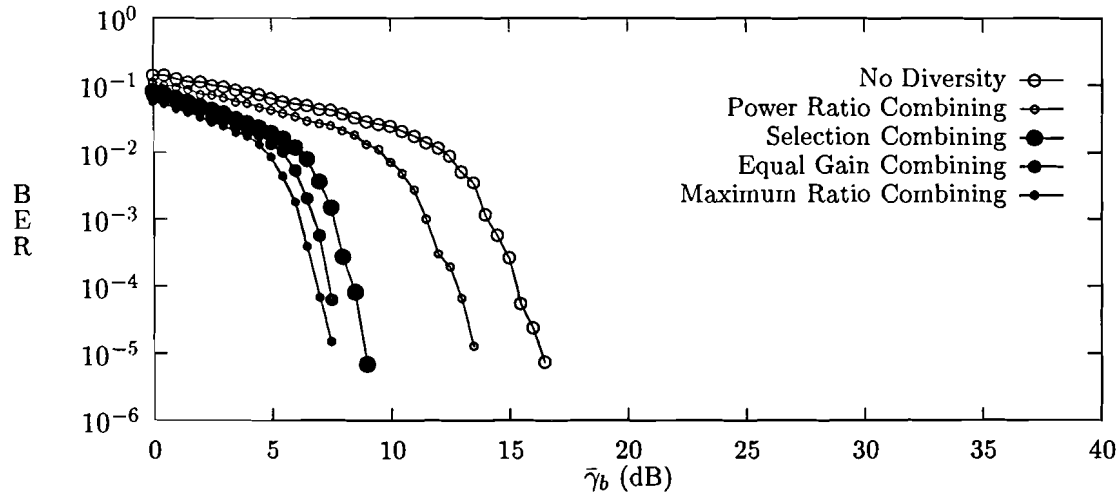

Figure 3.9: Performance of RS[255,223,33]-coded QPSK with $L = 2$ Antenna Diversity on an infinitely interleaved Rayleigh fading channel.

narrow-band combining technique. In the following chapters this will be worked out in detail.

Chapter 4

Channel Measurements

4.1 Introduction

From one of the buildings of Philips Research Labs in Eindhoven, an vertically polarized OFDM signal with an effective bandwidth B_{eff} of 7 MHz is being transmitted at a center frequency of 762 MHz. The characteristics of the OFDM transmitter are depicted in Appendix C. Because an OFDM spectrum is a flat spectrum, it is well suited for measuring fading characteristics. A PAL spectrum in contrary, has a few peeks at the specific frequencies. Before measurements of the received signal strength at different locations could be performed, there was need for an antenna system with which these measurements could take place. The following demands where made for the antenna system: At different locations we should be able to receive the transmitted OFDM spectrum with two different antennas. The distance between these antennas must be variable. Further, the received wide-band power spectrum of the OFDM signal must be stored on a computer. Some aspects of the antenna system will be discussed in this chapter.

4.2 Measurement setup

Because of the fact that measurements had to be carried out at many different locations, the measurement-setup had to be movable. A small car was used to carry all the equipment around. Figure 4.1 shows the system with which the measurements were carried out. The

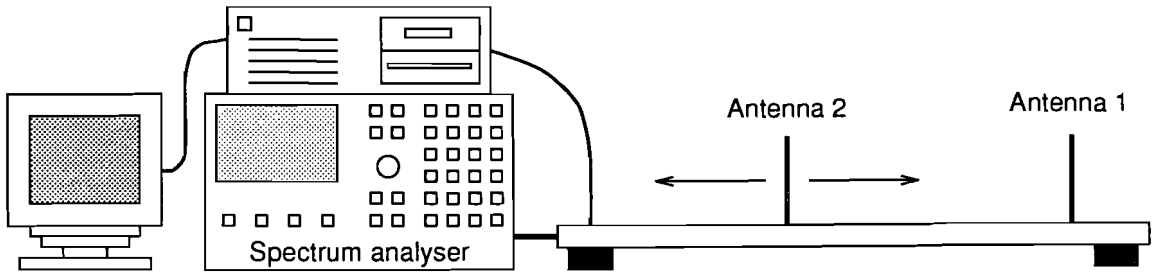

Figure 4.1: The measurement system

antennas used to receive the 7 MHz wide OFDM spectrum, are $\lambda/4$ mono-poles with a groundplane (see Appendix B). A large metal plate is used as ground-plane. Both antennas are vertically polarized. The computer is used as control-unit. With a little motor, antenna 2 can be moved very precisely over a distance of about 1 meter to vary the antenna spacing. The spectrum analyzer can measure the power spectra of the transmitted OFDM signal. This signal can be sent to a computer and stored on a harddisk.

4.3 The measurements

To obtain representative results it is necessary to measure the OFDM spectrum at many different locations. The locations were taken all over Eindhoven. Measurements were carried out in a large number of office-buildings, residential houses and apartment buildings within the range of the transmitter. Multiple measurements per location were carried out. In residential houses, for example, measurements where carried out in the living room, kitchen and other rooms that were reachable with the measurement setup. In the office buildings many measurements were carried out in different rooms and floors. For a complete overview of the locations where measurements were carried out see Appendix D.

During a measurement run, the setup was placed at a fixed position, while antenna 2 was moved to vary the distance between the two antennas. The initial spacing of the two antennas was always 10 cm ($\approx \lambda/4$). During one measurement run, 50 spectra received from each antenna were measured and sent to the computer. After a spectrum was read, antenna 2 was moved each time over a distance of 1.25 cm ($\approx \lambda/32$). After 50 measurements the distance between the antennas was 71.25 cm. The measurements showed that under stationary conditions the two antennas did not influence each other, since antenna 1 received 50 identical frequency spectra.

During a period of three weeks, measurements were carried out at 40 different locations. At each location, a number of 3 to 8 measurement runs were carried out. Every measurement run was carried out at another place in the room. The setup was also placed at another angle towards the transmitter. This was done to obtain a representative set of measurements for each location. All rooms reachable at a certain location were visited. This gave a total of approximately 200 measurement runs. One month after the measurements were finished, a few locations were visited again to verify the earlier acquired data. Under stationary conditions we found the results to be the same.

Chapter 5

System simulations

In this chapter, simulation results are presented showing the difference in performance between several narrow-band and wide-band combining techniques with respect to no combining according to the measurement results. Because the simulations were very time consuming only maximum ratio and selection combining were investigated. Simulations have been carried out using different Reed Solomon codes and different frequency interleaving depths. The channel data obtained from the measurements described in Chapter 4 are used in the simulations.

5.1 Computer simulations

The transmission scheme discussed in Chapter 2 is simulated with the aid of a computer program. The main task of the computer simulations is to simulate the actual situation as good as possible. It is assumed that the guard interval is long enough to get rid of Inter Symbol Interference (ISI). The following demands were made for the computer simulations:

- Given a certain measured spectrum, a Reed Solomon code and a modulation technique (for example QPSK), the BER can be calculated as function of the E_s/N_0.
- Given two measured spectra, a Reed Solomon code, a modulation technique and a combining technique, the BER after decoding of the combined signal can be calculated as function of E_s/N_0.

5.1.1 The Simulation Software

In order to be able to calculate the bit error rate of a certain spectrum as a function of the signal-to-noise ratio of the measured signal, a complete computer program had to be developed to carry out the desired functions. Figure 5.1 shows the setup of the program. The different blocks are described below.

Random bit generator

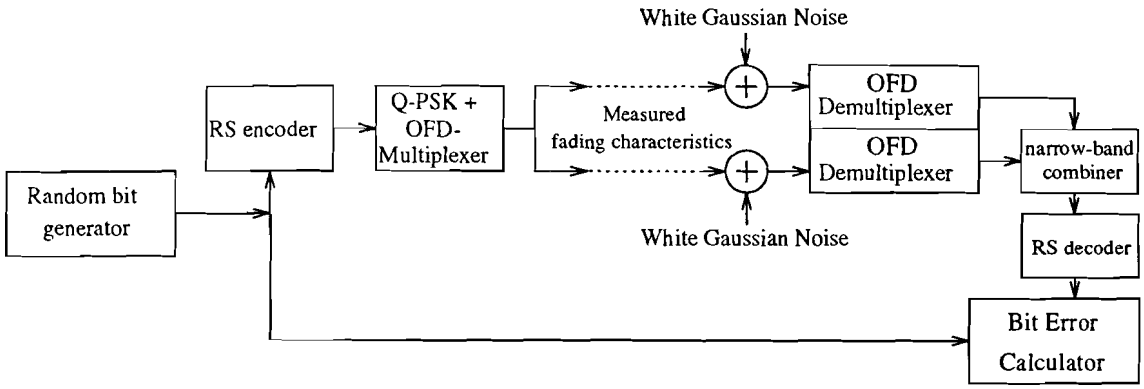

Figure 5.1: Simulation of narrow-band combining.

The random bit generator consists of a subroutine that produces randomly bits until a predetermined number of bit errors is detected.

Reed Solomon encoder

The generated bits are RS encoded. Unless stated otherwise, a RS[255,223,33] code was implemented, where one RS word consists of 1 byte. This byte in placed in 4 QPSK symbols in time. Unless stated otherwise, no interleaving is applied.

Modulator + OFD multiplexer.

The encoded bits are modulated according to a predetermined modulation technique and OFD multiplexed. The measured OFDM signal has a bandwidth of 7 MHz. If we place 1020 sub-channels in this 7 MHz wide signal, the sub-channel spacing becomes $f_s = B/1020 = 6.8$ kHz. In the rest of this report we will use this subchannel spacing and perform QPSK modulation on the subchannels.

Fading characteristics & Additive White Gaussian Noise

The OFDM spectra obtained from the measurements need to be implemented into the simulations. The wide-band measured OFDM spectra are divided into $N = 1020$ channels. The received signal of a kth OFDM channel becomes

$$r_k = \alpha_k s_k + n_k, \tag{5.1}$$

where $E[s_k s_k^*] = E_s$, $E[n_k n_k^*] = N_0$ and α_k is the attenuation factor of the kth OFDM subchannel. The α_k values can be calculated from the results of the measurements. This is done in the following way. Consider a received OFDM spectrum with 1020 sub-channels. The power received in a certain sub-channel k is P_k. The wide band received power of a measured OFDM spectrum becomes

$$P_{wide} = \sum_{k=1}^{N_{eff}} P_k \tag{5.2}$$

where P_k are values obtained from the measurements and $N_{eff} = 1020$. If we divide the wide-band received power by the number of OFDM channels we obtain the average received

power per OFDM channel ($\overline{P} = P_{wide}/N$). With the assumption that $E[\alpha_k \alpha_k^*] = 1$, the attenuation factor of a OFDM channel is calculated with

$$\alpha_k = \sqrt{\frac{P_k}{\overline{P}}} \tag{5.3}$$

These α_k values are real values. In an actual situation the value of α_k will be complex. Thus it is impossible to deduce from the measurement results, any phase information of the α_k. The received signal r_k is also disturbed by Additive White Gaussian Noise (with two-sided spectral density $N_0/2$). The noise power level can be varied in the simulations. This means that the average signal to noise ratio of the received (simulated) signal can be varied.

OFD Demultiplexer & narrow-band combiner

The disturbed signal is OFD Demultiplexed and combined in a narrow-band combiner. The narrow-band combiner can simulate different combining techniques such as maximum-ratio combining and selection combining. It is also possible to vary the combining bandwidth in terms of OFDM channels. The combiner generates a new improved signal with respect to no combining.

QPSK demodulator

The received symbols are converted to bits.

Reed Solomon decoder

We know from a RS[255,223,33] code that 16 byte errors can be corrected. The RS decoder looks at a data blok of 255 bytes. If more that 16 byte errors occur in this block, the RS decoder cannot correct the errors, otherwise all errors can be corrected.

Bit Error Calculator

The originally transmitted bits are compared with the bits that went through the simulated channel. The number of bit errors can be determined. The simulations stop when 250 byte errors have occurred. By varying the noise power N_0, the bit error rate (BER) can be calculated as a function of the average signal-to-noise ratio $\overline{\gamma_b}$ per information bit. For QPSK modulated bits, γ_b becomes

$$\overline{\gamma_b} = \frac{1}{2R}\frac{\overline{P}}{N_0} \tag{5.4}$$

where $R = 223/255$ is the code rate.

5.1.2 The Simulation Setup

This section briefly describes how the results are obtained with the simulations. As already stated, the simulator calculates the BER as a function of $\overline{\gamma_b}$. For example, if we use the measured spectra from Figure 3.7 in the simulator, we come up with the results of Figure

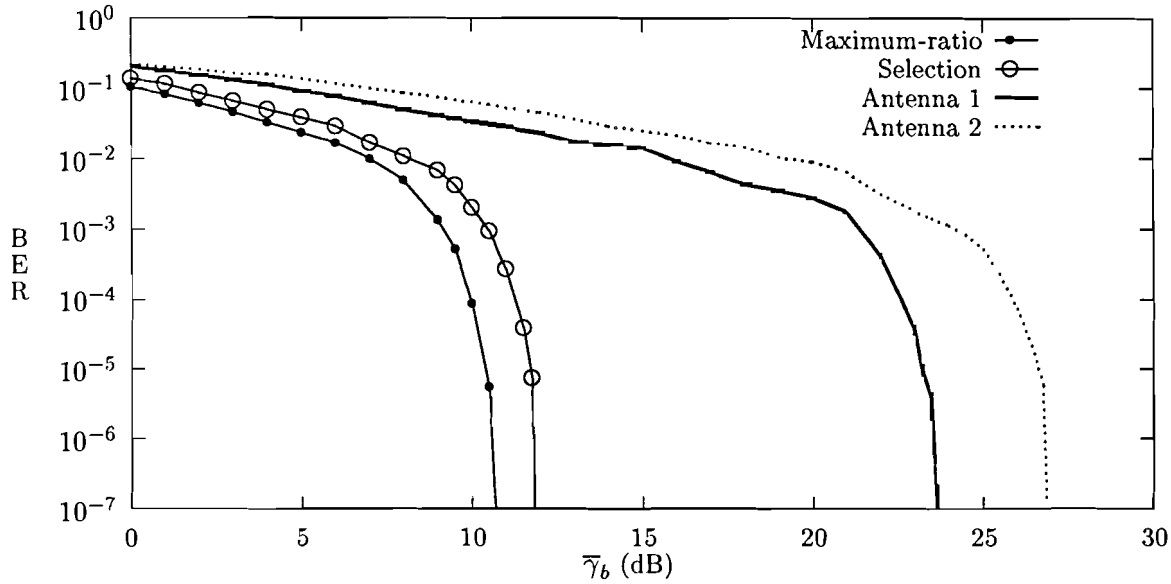

Figure 5.2: Simulation results for a RS[255,223,33] coded OFDM scheme for two narrowband combining techniques (2 antennas) and results when no combining is applied.

5.2. The results for both maximum ratio and selection combining are depicted. For bit error rates smaller than 10^{-4}, maximum ratio combining gives 1 dB extra performance improvement compared with selection combining. The performance of the system without antenna diversity is also depicted in Figure 5.2. For this particular situation the gain G (see equation 3.34) reached with selection combining would be 13 dB. Figure 5.2 illustrates only one simulation result. The gain G, as a function of the distance between the two antennas, is a more interesting measure. In Chapter 4 it was stated that each measurement run consisted of 50 measured spectra for each antenna. The gain as function of the antenna spacing for a certain measurement run can be calculated by using the measured spectrum of antenna 1 and combine it with any of the 50 measured spectra of antenna 2. Another possibility is to combine the mth measured spectrum (from a certain measurement run) of antenna 2 with all the other measured spectra of antenna 2 from the same measurement run. This leads to $M \times (M-1) = 50 \times 49$ extra pairs of measured spectra for each measurement run where simulations can be carried out with.

5.1.3 What can be derived from the simulations

The object of the simulations is to be able to come to some interesting conclusions about antenna diversity in relation to the OFDM system. The following items have been investigated:

- The average gain averaged over all visited locations that can be expected as a function of the distance between the two antennas.
- The distribution of this gain.
- The gain that can be expected at locations with poor reception conditions.

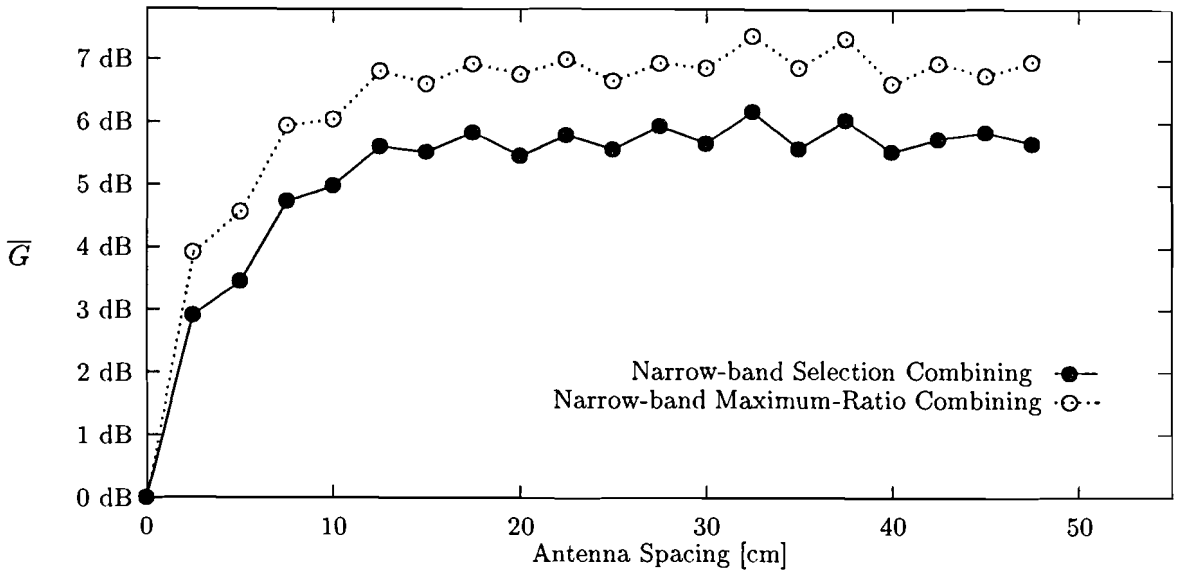

Figure 5.3: The average gain reached with selection combining and maximum-ratio combining as a function of the distance between the two antennas, for a RS[255,233,33] coded OFDM scheme (BER=10^{-4}; $\lambda = 39.4$ cm).

- The average gain that can be expected when the combining bandwidth is increased.
- Relation between coherence bandwidth and maximum useful combining bandwidth.
- The effect of different codes and different frequency interleaving depths on the performance of the combining techniques.

5.2 The Average Gain reached with selection combining and maximum ratio combining

A interesting measure for the performance improvement is the average gain $\overline{G}$ that can be achieved with narrow-band combining (based on the measurement results), with

$$\overline{G} = 10 \times \log\left(\frac{1}{Q}\sum_{k=1}^{Q} 10^{\frac{G}{10}}\right) \tag{5.5}$$

where Q is the number of simulation-runs. Figure 5.3 depicts the average gain achieved with selection combining and maximum-ratio combining as a function of the distance between the antennas. The combining was carried out for each OFDM subchannel separately. In this particular Figure, $\overline{G}$ is an average for all locations where measurements have been carried out.

In Figure 5.3 it can be seen that the antenna spacing is of importance. If the antenna spacing is larger than 10 cm ($\frac{\lambda}{4}$), $\overline{G}$ has reached its maximum value for both combining

techniques. From this we can deduct that the signals received at an antenna are sufficiently uncorrelated when the antenna spacing is larger than $\frac{\lambda}{4}$. With Figure 5.3 it can be seen that $\overline{G}$ is 5.5 dB for selection combining and 6.7 dB for maximum-ratio combining. In Section 3.4 was found that maximum ratio improves the reception quality, in comparison with selection combining, with approximately 1.3 dB, when $L = 2$ antennas were used. The simulation results show the same effect, provided that only the simulation results where the antenna spacing is larger than $\frac{\lambda}{4}$ are taken into account.

Another interesting results is the distribution of G. The distribution gives information about the percentage of locations where G is below a threshold value. Only those simulation results where the antenna spacing is larger than $\frac{\lambda}{2}$ are taken into account. Figure 5.4 shows the probability density function of G for both maximum-ratio and selection combining. This figure permits us to calculate the probability that a certain threshold gain is exceeded (probability distribution function). Figure 5.5 illustrates this.

The results depicted until now, were based on all measurements. It is much more interesting to know what gain G will be obtained for locations with poor reception conditions. For example, it is possible to take a subset of all measurement locations where the following demands were made for those locations:

- Houses at large distance from the transmitter (at least 5 km).
- Locations deep inside buildings (e.g. inside the University of Technology)
- House and apartment buildings with large obstacles between transmitter and receiver.

Figure 5.6 depicts the average gain $\overline{G}$ for those locations. It can be seen that much higher performance improvement can be reached when the reception conditions are poor (9 dB for selection combining and 10 dB for maximum-ratio combining). From Figure 5.6 we can depict that the locations that need this extra improvement, benefit more from antenna diversity than location with good reception conditions.

5.3 Increasing the combining bandwidth

Until now it was assumed that the combining took place for each OFDM subchannel separately. Such a combiner has a large hardware complexity (Chapter 6). To reduce complexity we can increase the combining bandwidth. For an OFDM scheme, the OFDM subchannels are obtained with a FFT. Normally, for $L = 2$ antenna diversity, two of these FFT operations are needed. Because it is also possible to perform the combining somewhere inside the FFT, complexity is reduced. Practically this means that the combining in not carried out for each OFDM subchannel separately, but for a group of OFDM-channels as being one. Increasing the combining bandwidth has two disadvantages. First, it is more difficult to use maximum-ratio combining (because it becomes more difficult to define $\alpha_{j,i}$). Secondly, if the combining bandwidth is increased, this will normally reduce the performance improvement.

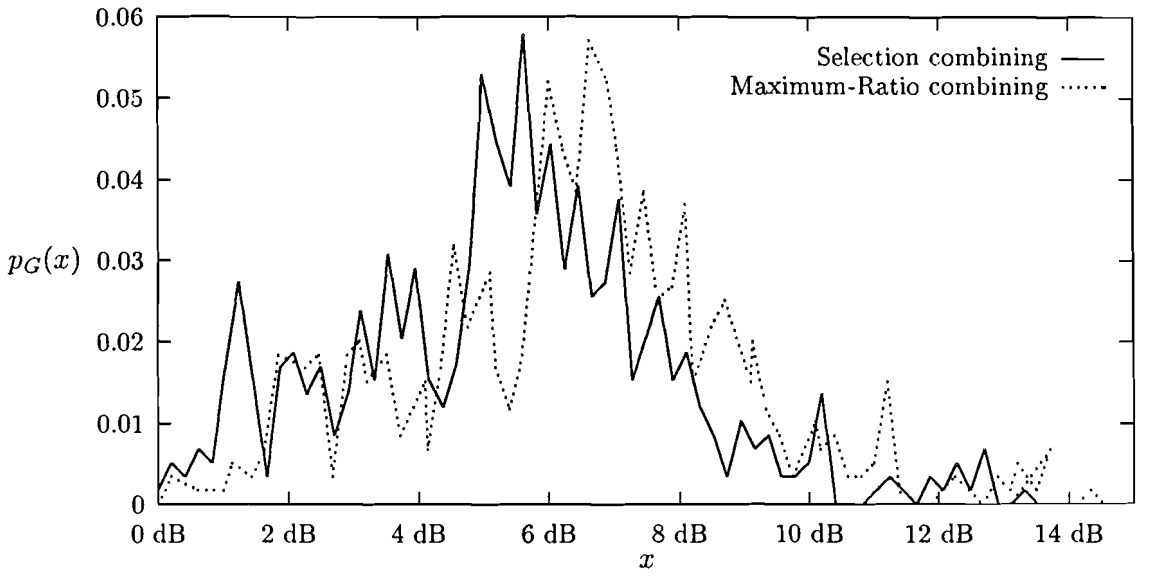

Figure 5.4: Probability density function of G for a RS[255,223,33] coded OFDM scheme.

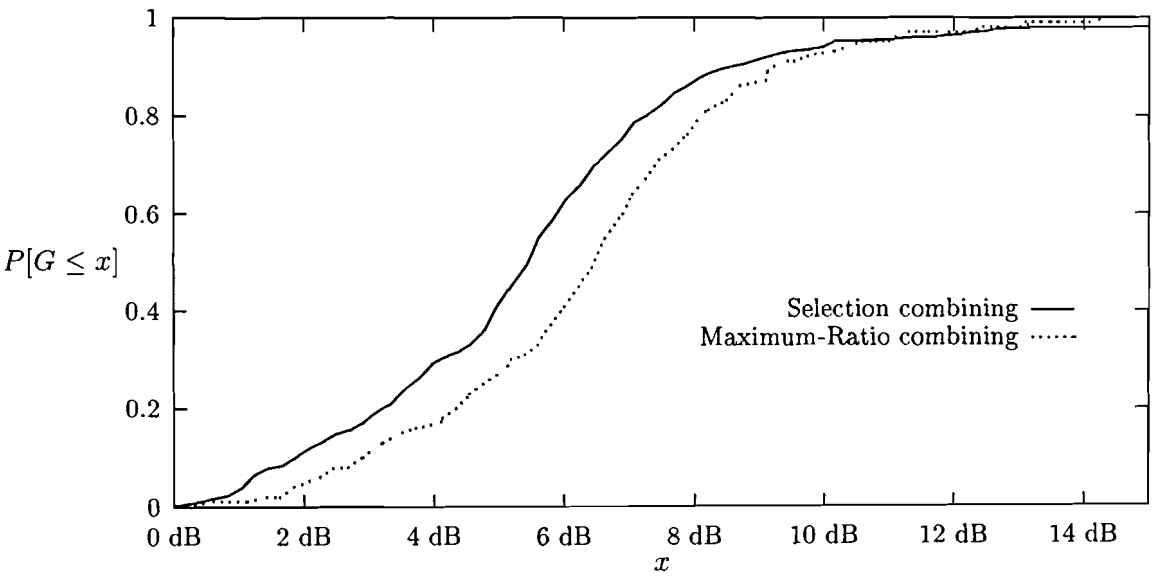

Figure 5.5: Probability distribution function of G for a RS[255,223,33] coded OFDM scheme.

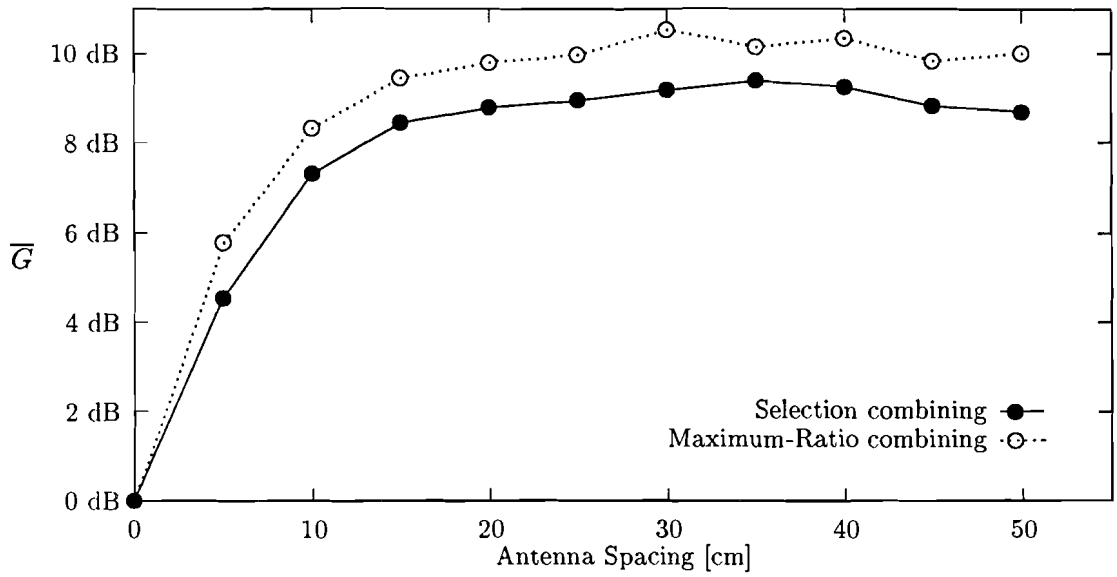

Figure 5.6: The average gain reached with two combining techniques as a function of the distance between the two antennas, for locations with poor reception conditions on a RS[255,223,33] coded OFDM scheme (BER=10^{-4}; $\lambda = 39.4$ cm).

For selection combining, an increasing combining bandwidth means no more than selecting the cluster of OFDM subchannels with the strongest received power. Figure 5.7 illustrates the average achieved gain with selection combining for different combining bandwidths, where all measurement locations were taken into account. It can be seen that $\overline{G}$ decreases when more subchannels are combined together. The gain that can be expected for a certain combining bandwidth is also dependent on the coherence bandwidth. If the combining bandwidth becomes larger than the coherence bandwidth, the expected gain will decrease rapidly. On the other hand, at locations where the reception conditions are reasonably good, the largest distortion will come from short (strong) echoes. In this case we will have a large coherence bandwidth and the received signal will be frequency non-selective. Wide-band combining will still result in much gain for these locations.

Locations with poor reception conditions suffer much more from longer echoes. The received signal will be very frequency selective and the difference in performance between narrow-band and wide-band combining will be much higher. Figure 5.8 illustrates this.

5.4 Usage of different codes and frequency interleaving depths

The simulation results presented until now where based an a RS[255,223,33] code with no frequency interleaving. Normally, when a RS code is applied, the code-words belonging to a code will be interleaved in frequency. Figure 5.9 illustrates this for a RS[255,223,33]

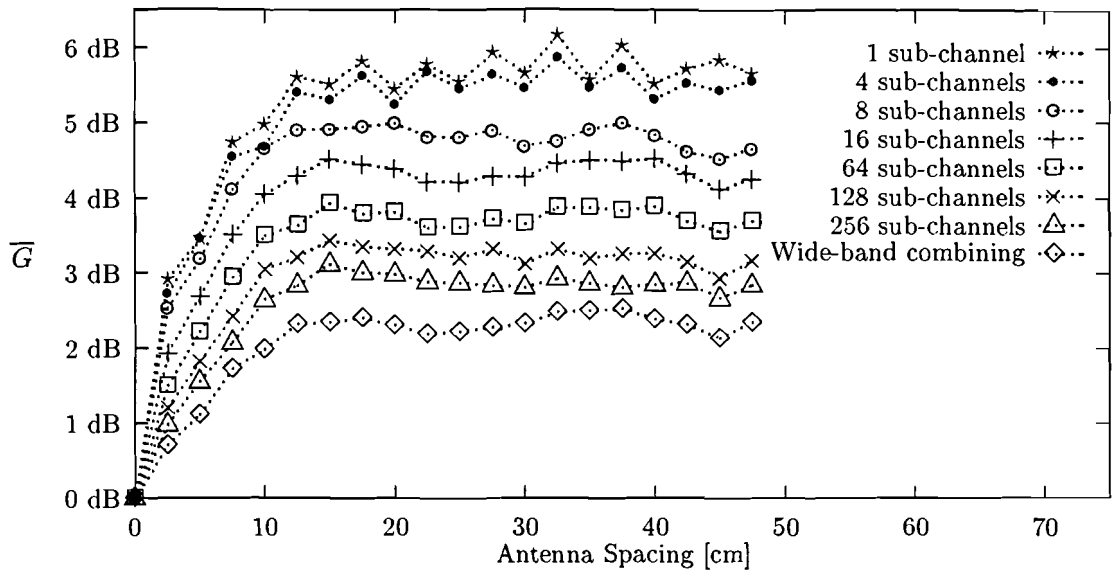

Figure 5.7: The average gain (for all locations), achieved with selection combining as a function of the distance between the two antennas, for an increasing combining bandwidth for a RS[255,223,33] coded OFDM scheme (BER=10^{-4}; λ=39.4 cm).

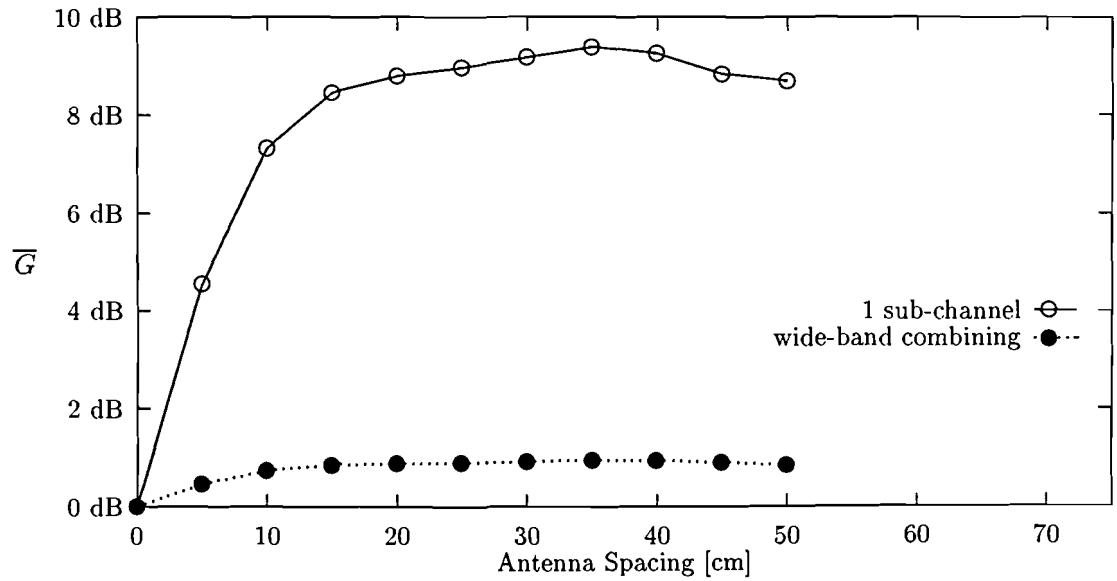

Figure 5.8: The average gain (for locations with poor reception conditions), achieved with selection combining as a function of the distance between the two antennas, for narrow-band and wide-band combining for a RS[255,223,33] coded OFDM scheme (BER=10^{-4}; λ=39.4 cm).

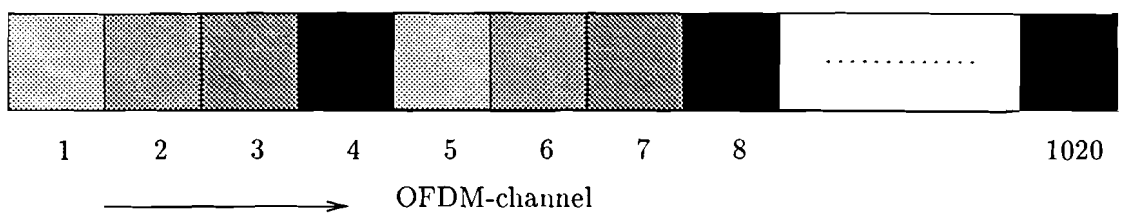

Figure 5.9: RS coding with frequency interleaving, the parts with the same shades belong to the same code.

code. If a RS[255,223,33] code is applied (with 1020 OFDM-channels), 4 frequency interleaving can be implemented. If frequency interleaving is applied, the RS code will improve the performance (with respect to no frequency interleaving) because two successive code-words will be less correlated and the less correlation between code-words, the better the performance of the code. Figure 5.10 shows the difference in performance improvement with narrow-band selection and maximum-ratio combining for a RS[255,223,33] code when four frequency interleaving is applied and without frequency interleaving. It can be seen from Figure 5.10 that $\overline{G}$ decreases when interleaving is applied. This is obvious because the RS code gives better results when frequency interleaving is applied. We can conclude from this that the performance improvement, when antenna diversity is applied, decreases when the performance of the RS code increases (and vise versa).

Figure 5.11 illustrates that the overall performance improves when frequency interleaving is applied. This Figure also illustrated the reason why $\overline{G}$ decreases when frequency interleaving is applied.

Simulations have also been carried out using another RS code. A fictive code was used with a length of 1020 code words. From the set of 1020 code words, 16 word errors can be corrected (for simplicity we call this a RS[1020,988,33] code. The RS[255,223,33] code on the other hand, can correct 16 word errors in a block of 255 words. It can be expected that the RS[255,223,33] code has a higher performance. If we carry out simulations with the RS[1020,988,33] code we find the average gain $\overline{G}$ to be 1.1 dB higher when selection combining is used as combining technique.

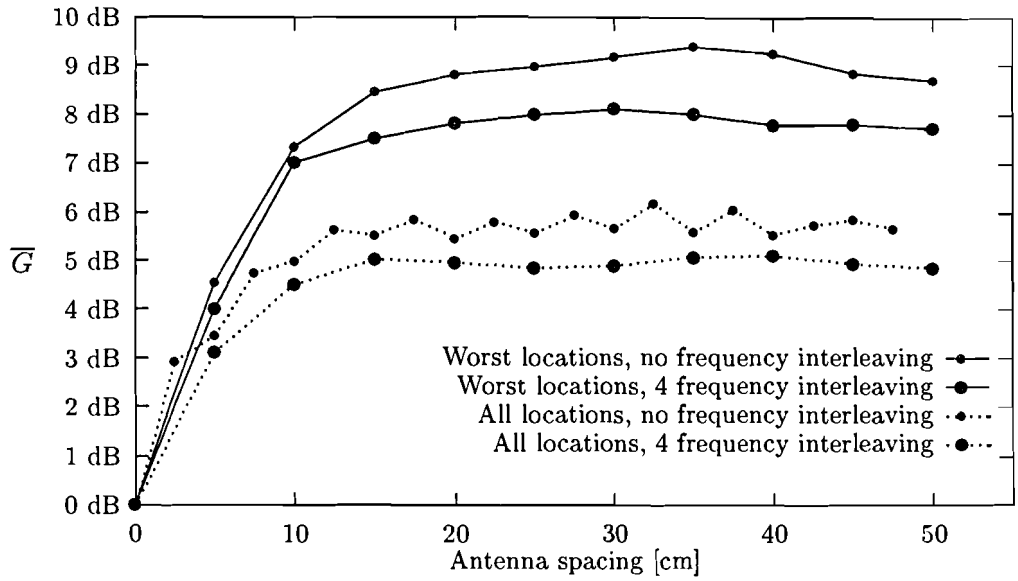

Figure 5.10: Simulation results for selection combining, with and without frequency interleaving, as a function of the distance between the two antennas, for a RS[255,223,33] coded OFDM scheme (BER=10^{-4}; $\lambda = 39.4$ cm).

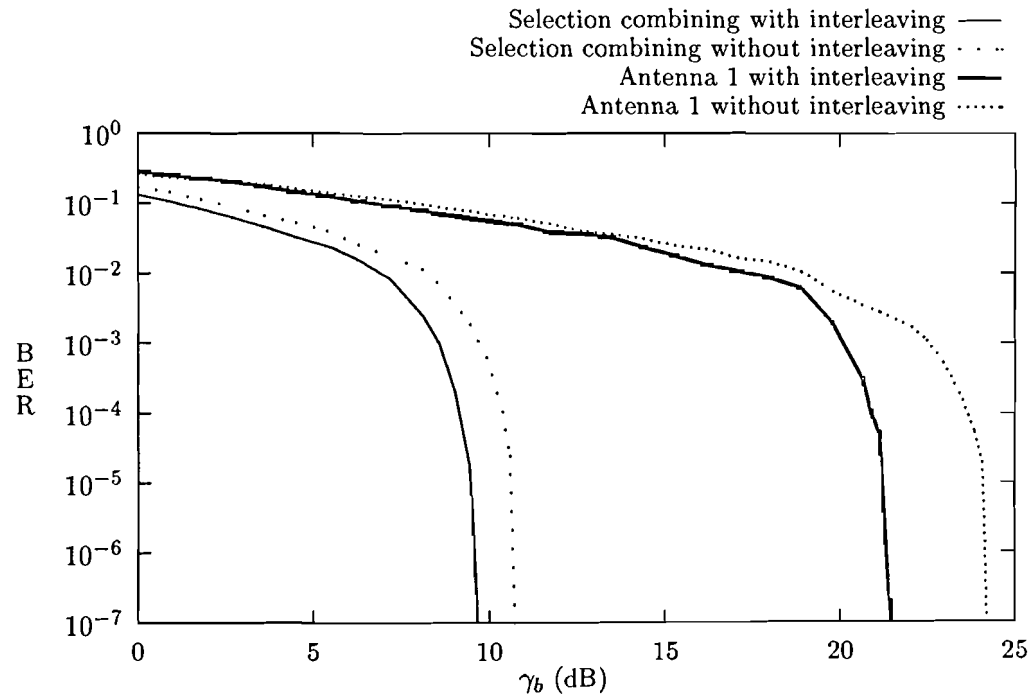

Figure 5.11: One simulation result, showing the difference in performance between interleaving and no interleaving, with and without selection combining.

Chapter 6

Hardware implementation

Implementing a diversity system for an OFDM based scheme into hardware adds complexity to the traditional hardware implementation for an OFDM scheme. Normally, for $L = 2$ antenna diversity, we need two complete frond-ends and two FFT chips. These components are at this moment still very expensive.

A frond-end which convert the HF signal to a base-band signal contains a very stable oscillator. This oscillator could probably be shared by both frond-ends, and hence leads to reduced costs. The same holds for the frequency and time synchronization units.

The FFT operation, on the other hand, should normally be performed twice. In Section 5.3 is shown that increasing the combining bandwidth reduces complexity. In Section 5.3, it was also shown that the performance of the diversity system decreases with increasing combining bandwidth. The measure of performance decreasement that is acceptable, is something that only can be determined with experiments.

There is however a possibility to implement both FFT operations of a diversity system with only one FFT chip, if this chip is sufficiently fast. A requirement for this chip is that it can calculate two complete Fourier transforms during the duration of a single symbol including the guard interval. A possible hardware implementation for a diversity scheme using only one FFT chip is shown in Figure 6.1. Problems related with timing and frond-ends are not yet considered.

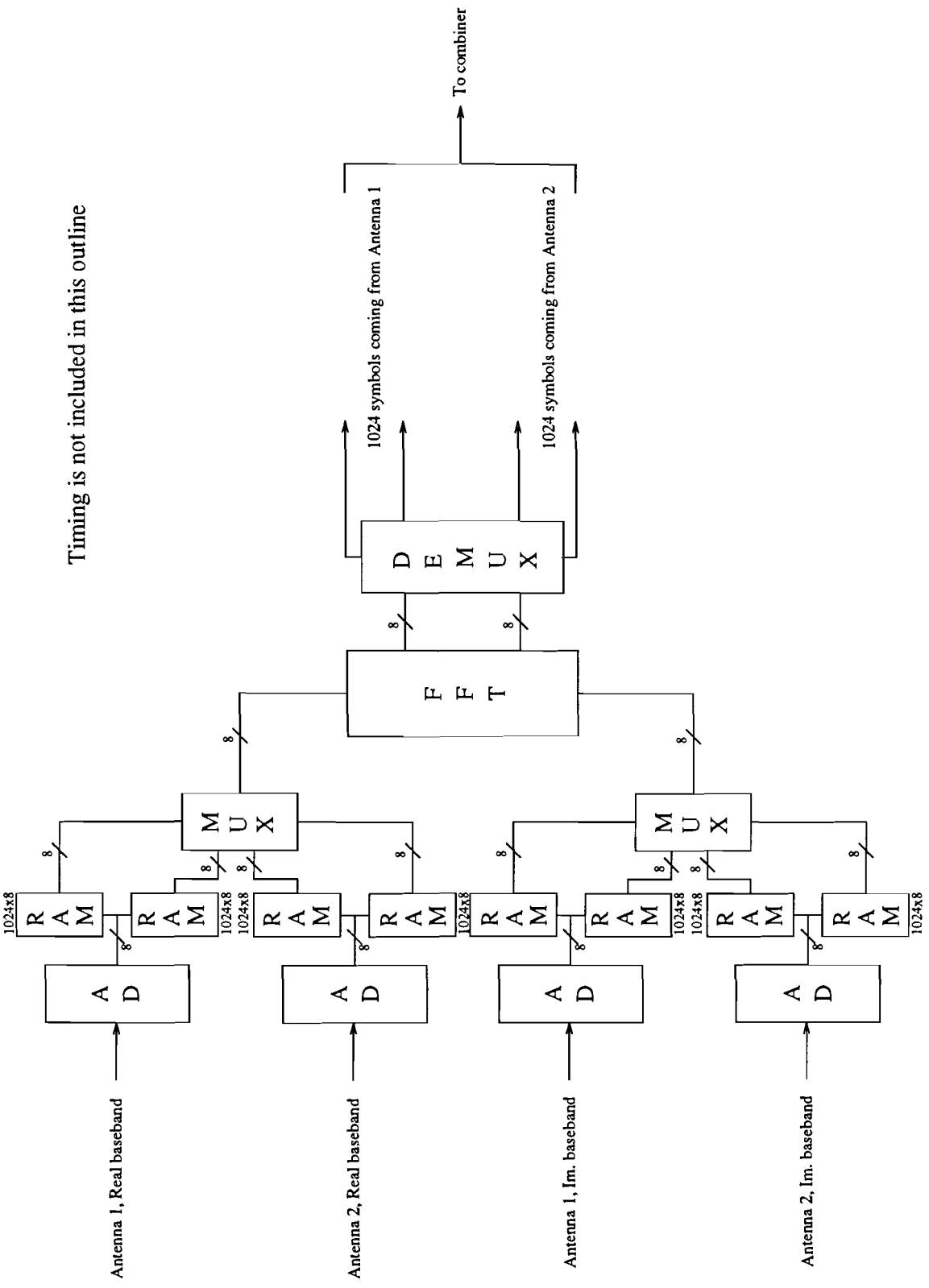

Figure 6.1: Possible hardware implementation for a diversity system

Chapter 7

Conclusions

In this chapter some conclusions are formulated with respect to the research that has been carried out. First, some traditional combining techniques were discussed. Further, the perfomances of these combining techniques in combination with a coded OFDM scheme are discussed. It will be shown that the choice of the code is of importance for the performance improvement when antenna diversity is applied. The choice of the combining bandwidth is also of importance.

In Section 3.4 it was shown that the performance improvement of a diversity system is very dependent on the applied combining technique. We saw that combining techniques that take into account the phase information of the received signals, such as maximum-ratio combining and equal gain combining, resulted in a high performance improvement. Combining techniques that do not use the phase information of the received signal gave very little performance improvement. Selection combining, is a combining technique that doesn't fall into these categories. It can compete very well with maximum-ratio and equal gain combining when L is small.

The performance improvement of maximum-ratio, equal gain (has not been investigated) and selection combining, when used in a coded OFDM scheme, is also very high, presumed the combining can take place for each OFDM subchannel separately. With maximum-ratio combining, an average gain of 7 dB was found (based on all the measurements). It was also found that the spacing of the antennas is of importance. When the antenna spacing was larger than $\frac{\lambda}{4}$, the received signals at both antennas were sufficiently uncorrelated.

The performance improvement at locations with poor reception conditions was even higher. Maximum-ratio combining gave an average gain of 10 dB for these locations.

The combining bandwidth is also important for the performance improvement. It is obvious that when the coherence bandwidth is much larger than the combining bandwidth, the best result are to be expected with antenna diversity. Locations with poor reception conditions, usually have a very small coherence bandwidth. Increasing the combining bandwidth will rapidly decrease the performance of antenna diversity for these locations.

The choice of code and the frequency interleaving depth are also of importance for the

performance of antenna diversity. If a code is used with very good performances, antenna diversity can add some extra improvement to the performance. This extra improvement becomes smaller when a better code is used and visa versa.

Chapter 8

Suggestions for further research

In this report simulation results of the gain that can be expected when antenna diversity is applied where presented. Antenna diversity increases the performance of a coded OFDM system considerably. But to obtain more representative results we can make some suggestions:

- Given the performance improvement, based on measurements and simulation results, it would be very useful to implement a diversity system into hardware. Because an OFDM modem and an MPEG encoder and decoder already exist, this should not be that difficult. When a diversity system is built, the performance can be measured much more effective. One can compare the relative time that the picture quality is unacceptable with and without antenna diversity.
- The measurements carried out for the simulations could only take place in Eindhoven because the transmitter power was not strong enough to carry out measurements further away from the transmitter. It is however very interesting to investigate the results of antenna diversity when the distance between the transmitter and receiver becomes larger, because most likely the echoes will become longer if the distance between transmitter and receiver becomes larger. The longer the echoes, the smaller the coherence bandwidth and the smaller the coherence bandwidth the more the received signal suffers from frequency selectivity.
- It can be very interesting to calculate the performance improvement instead of simulating this. During the research period, an effort has been done to calculate the performance improvement with a certain recursive algorithm, but this algorithm required too much computer time. It can be interesting to improve the speed of this algorithm.

As mentioned above, there is still a lot of work that can be carried out on the area of antenna diversity. Of course what will and won't be carried out is a matter of costs and priority.

Bibliography

[1] M. Abramowitz and I.A. Stegun ed. *Handbook of Mathematical Functions.* Dover, New York NY, 1965.

[2] M. Alard and R. Lassalle. Principles of modulation and channel coding for digital broadcasting for mobile receivers. *EBU Review*, (224):168–190, August 1987.

[3] J. Been. Antenna diversity: another way to improve car radio reception. Technical report, Customer Support Group Nijmegen - The Netherlands, November 1988. (Application note).

[4] J. Been. Antenna diversity with the TEA 6101 and the TDA 1596 and the car radio design-in. Technical report, Customer Support Group Nijmegen - The Netherlands, April 1989. (Application note).

[5] H. H. Beverage and H. O. Peterson. Diversity receiving system of r.c.a. communications, inc., for radiotelegraphy. *Proceedings of the I.R.E.*, 19:531–561, April 1931.

[6] P.G.M. de Bot. Antenna diversity for OFDM systems. In *Proc. Symp. on Information Theory in the Benelux*, pages 244–251, Veldhoven, The Netherlands, May 1993.

[7] P.G.M. de Bot and A.J.M. Wijlaars. Measurement on indoor reception of broadcast signals. Technical Report UR 029/92, Philips Research Laboratories Eindhoven, Eindhoven, The Netherlands, November 1992. (dTTb/WP5/024/92, available on request).

[8] P.G.M. de Bot, Antoine J.M. Wijlaars, and Hans Kollenbrander. Measurements on indoor reception of digital broadcast signals at 762 mhz. Technical Report UR 016/93, Philips Research Laboratories Eindhoven, Eindhoven, The Netherlands, September 1993.

[9] P.G.M. de Bot C.P.M.J. Baggen, A. Chouly, and A. Brajal. An example of a multi-resolution digital terrestrial TV modem. In *Proc. Int. Conference on Communications*, pages 1785–1790, Geneva, Switzerland, May 1993.

[10] D.G. Brennan. Linear diversity combining techniques. *Proc. IRE*, 47(6):1075–1102, June 1959.

[11] T.M. Cover. Broadcast channels. *IEEE Trans. Information Theory*, IT-18(1):2–14, January 1972.

[12] A. de Haas. Short-wave reception without fading. *Radio-Nieuws*, (12):357–364, December 1927. (In Dutch).

[13] A. de Haas. Short-wave reception without fading II. *Radio-Nieuws*, (2):80–88, February 1928. (In Dutch).

[14] M. Failli. Digital land mobile radio communications. Technical report, Commission of the European Communities, COST 207 Management Committee, September 1984.

[15] W.C. Jakes. *Microwave Mobile Communications.* Wiley, 1974.

[16] J.G.W.M. Janssen, P.G.M. de Bot, and A.J.M. Wijlaars. Antenna diversity for digital video broadcasting. In *IEEE First Symposium on Communications and Vehicular Technology in the Benelux*, pages 6.4.1–6.4.8, Delft, The Netherlands, October 1993.

[17] K. Lohse. Besserer radio-empfang im fahrenden auto. *Funkschau*, 4/1993:56–59, April 1993.

[18] F.J. MacWilliams and N.J.A. Sloane. *The Theory of Error-Correcting Codes.* North Holland, Amsterdam, 1977.

[19] A.J. Motley and S.E. Alexander. Diversity advantage for cordless telephones. *Electronics Letters*, 19(14):531–533, July 1983.

[20] H. O. Peterson, H. H. Beverage, and J. B. Moore. Diversity telephone receiving system of r.c.a. communications, inc. *Proceedings of the I.R.E.*, 19:562–584, April 1931.

[21] Philips. Service manual for car vision receiver box, 1989.

[22] J.G. Proakis. *Digital Communications.* McGraw-Hill, Singapore, second edition, 1989.

[23] W.L. Stutzman and G.A. Thiele. *Antenna theory and design.* Wiley, New York, 1981.

[24] S.B. Weinstein and P.M. Ebert. Data transmission by frequency-division multiplexing using the discrete fourier transform. *IEEE Trans. Communications*, COM-19(5):628–634, October 1971.

[25] J.M. Wozencraft and I.M. Jacobs. *Principles of Communication Engineering.* Wiley, New York NY, 1965.

Appendix A

The Rayleigh distribution

Consider two independent real stochastical variables x and y, each Gaussian distributed with $E[x] = E[y] = 0$ and standard deviation $E[x^2] = E[y^2] = \sigma^2$. The joint probability density function is given by:

$$f(x,y) = f(x) \cdot f(y) = \frac{1}{2\pi\sigma^2} e^{\left(\frac{-(x^2+y^2)}{2\sigma^2}\right)} \tag{A.1}$$

If we express (A.1) in polar coordinates (r, θ), where

$$r^2 = x^2 + y^2$$

$$\theta = \arg(x + jy)$$

and

$$\mathrm{d}x\mathrm{d}y = r\mathrm{d}r\mathrm{d}\theta$$

The probability density function in coordinates r and θ, $g(r,\theta)$ follows from

$$g(r,\theta)\mathrm{d}r\mathrm{d}\theta = f(x,y)\mathrm{d}x\mathrm{d}y$$

and becomes

$$g(r,\theta) = \frac{r}{2\pi\sigma^2} e^{\left(\frac{-r^2}{2\sigma^2}\right)} \tag{A.2}$$

The probability density function of the phase θ can be calculated by integrating r over $[0,\infty\rangle$ and substituting $u = r^2/2\sigma^2$

$$g(\theta) = \frac{1}{2\pi\sigma^2} \int_0^\infty r e^{\left(\frac{-r^2}{2\sigma^2}\right)} \mathrm{d}r = \frac{1}{2\pi} \int_0^\infty e^{-u} \mathrm{d}u = \frac{1}{2\pi}, \quad |\theta| \leq \pi. \tag{A.3}$$

Hence, the phase θ is uniformly distributed over $(-\pi, \pi)$. In the same way as we calculated the density function for the phase, we can calculate the probability density function $g(r)$ for the amplitude r,

$$g(r) = \int_{-\pi}^{\pi} g(r,\theta)\mathrm{d}\theta = \frac{r}{\sigma^2} e^{-r^2/2\sigma^2}, \quad r \geq 0 \tag{A.4}$$

r is defined to be Rayleigh distributed and equation (A.4) gives the Rayleigh probability density function.

The expectation of r^k

The expectation $E[r^k]$ of r^k follows from [22]:

$$E[r^k] = \int_0^\infty r^k \, g(r) \mathrm{d}r \tag{A.5}$$

With the aid of the Gamma function $\Gamma(p)$ [22], where

$$\Gamma(p) = \int_0^\infty t^{p-1} e^{-t} dt \qquad p > 0$$

$$\Gamma(p) = (p-1)! \quad p \text{ an integer, } p > 0$$

$$\Gamma\left(\frac{1}{2}\right) = \sqrt{\pi}$$

$$\Gamma\left(\frac{3}{2}\right) = \frac{\sqrt{\pi}}{2}$$

$E[r^k]$ becomes

$$E[r^k] = (2\sigma^2)^{k/2} \Gamma\left(\frac{k+2}{2}\right) \tag{A.6}$$

Appendix B

The antenna

Before it's possible to begin any signal strength measurements you need to have an antenna. Antennas can be divided in two groups: linear antennas and aperture antennas. In the next Sections, the Maxwell equations will be used. The reader is assumed to be familiar with these equations.

B.1 Characteristics of the ideal dipole antenna

The ideal dipole is a fictive antenna, but may be considered to be a piece of a larger current on an actual antenna. We shall use the term ideal dipole for a piece of uniform amplitude current which is of infinitesimal length or of very small finite length, $\Delta z \ll \lambda$. Consider an element of current of length Δz along the z-axis, centered on the coordinate origin. The current is of constant amplitude I. The current density can be represented by

$$\mathbf{J} = I\,\delta(x')\,\delta(y')\,\hat{\mathbf{z}} \quad for \quad -\frac{\Delta z}{2} < z' < \frac{\Delta z}{2} \tag{B.1}$$

In this case the vector potential volume integral (see appendix ?) reduces to a one-dimensional integral.

$$\mathbf{A} = \hat{\mathbf{z}}\mathbf{I} \int_{-\Delta z/2}^{\Delta z/2} \frac{e^{j\beta R}}{4\pi R}\, dz' \tag{B.2}$$

The length Δz is very small compared to the wavelength λ and the distance R. See Fig B.1. Since Δz is very small, the distance R from points on the current element to the field point equals the distance r from the origin to the field point. Substituting r for R in (B.2) and integrating gives

$$\mathbf{A} = \frac{Ie^{-j\beta r}}{4\pi r}\,\Delta z\,\hat{\mathbf{z}} \tag{B.3}$$

For an infinitesimal current, (B.3) is exactly true and is approximately true for a small ($\Delta z \ll \lambda$ and $\Delta z \ll R$) but finite uniform current element. We are now ready to calculate the electromagnetic fields created by the ideal dipole. The magnetic field becomes [23]

$$\mathbf{H} = \nabla \times \mathbf{A} = \nabla \times (A_z \hat{\mathbf{z}}) \tag{B.4}$$

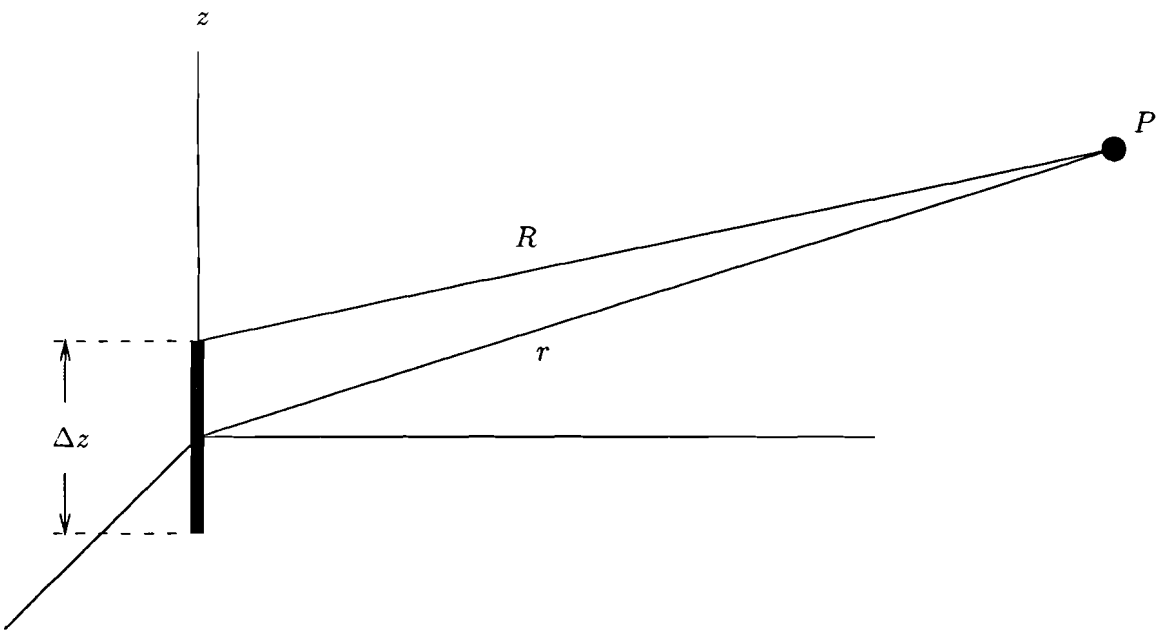

Figure B.1: The ideal dipole. Current I is uniform, $\Delta z \ll \lambda$, and $R \approx r$.

and the electrical field

$$\mathbf{E} = \frac{1}{j\omega\varepsilon} \nabla \times \mathbf{H} \tag{B.5}$$

If we only look at the electric and magnetic fields far away ($r \gg \lambda$), the magnetic and electrical fields become respectively,

$$\mathbf{H} = \frac{I\Delta z}{4\pi} j\beta \frac{e^{j\beta r}}{r} \sin\theta \hat{\Phi} \tag{B.6}$$

$$\mathbf{E} = \frac{I\Delta z}{4\pi} j\omega\mu \frac{e^{j\beta r}}{r} \sin\theta \hat{\Theta} \tag{B.7}$$

B.1.1 Directivity and Gain

One very important description of an antenna is how much it concentrates energy in one direction in preference to radiation in other directions. This characteristic of an antenna is called directivity and is equal to its power gain if the antenna is 100% efficient. Usually power gain is expressed relative to a reference such as an isotropic radiator or half-wavelength dipole. The power radiated by an antenna is

$$P_r = \frac{1}{2} Re \int\int (\mathbf{E} \times \mathbf{H}^*) \cdot d\mathbf{s} \tag{B.8}$$

In the far field of the antenna, where $\mathbf{E}$ and $\mathbf{H}$ are in phase, perpendicular and in a plane perpendicular on the propagation direction, the powerflux $S(R, \theta, \phi)$ is

$$S(R, \theta, \phi) = \frac{1}{2} \left| \frac{E^2(R, \theta, \phi)}{120\pi} \right| \quad Watt/m_2 \tag{B.9}$$

This means that the power per steradian can be defined as

$$P(\theta,\phi) = R^2 \times S(R,\theta,\phi) = \frac{1}{2}R^2 \left| \frac{E^2(R,\theta,\phi)}{120\pi} \right| \tag{B.10}$$

If we integrate $P(\theta,\phi)$ over all angles around the antenna we obtain the total radiated power

$$P_r = \int_0^{\pi} \int_0^{2\pi} P(\theta,\phi) \sin\theta \, d\theta \, d\phi \tag{B.11}$$

The radiation intensity $P_i(\theta,\phi)$ of an isotropic radiator is $P_i(\theta,\phi) = \frac{P_r}{4\pi}$.

Definition 1 *The gain function $G(\theta,\phi)$ of an antenna, in the far field, is defined as the relation between the radiation intensity of an antenna and the radiation intensity $P_i(\theta,\phi)$ of an isotropic radiator.*

$$G(\theta,\phi) = \frac{P(\theta,\phi)}{P_i(\theta,\phi)} = \frac{4\pi P(\theta,\phi)}{P_r} \tag{B.12}$$

Definition 2 *The maximum of the gain function $G(\theta,\phi)$ is called the antenna gain G.*

Let us consider the ideal dipole again. If equation (B.6) and (B.7) are used in equation (B.8) and the integral is calculated we find

$$P_r = -\int_0^{\pi} \int_0^{2\pi} \left[\frac{I\Delta z}{4\pi} j\omega\mu \frac{e^{j\beta r}}{r} \sin\theta \right] \times \left[\frac{I\Delta z}{4\pi} j\beta \frac{e^{j\beta r}}{r} \sin\theta \right] R^2 \sin\theta d\theta d\phi \tag{B.13}$$

$$P_r = \frac{\beta\omega\mu(I\Delta z)^2}{12\pi} = \frac{4\pi}{3}\left(\frac{I\Delta z}{4\pi}\right)^2 \beta\omega\mu \tag{B.14}$$

With equation (B.10) we find

$$P(\theta,\phi) = \frac{1}{2}\left(\frac{I\Delta z}{4\pi}\right)^2 \beta\omega\mu \sin^2\theta \tag{B.15}$$

With both the expressions for P_r and $P(\theta,\phi)$ we can calculate the antenna gain function for the ideal dipole antenna.

$$G(\theta,\phi) = \frac{3}{2}\sin^2\theta \tag{B.16}$$

And this implies that the antenna gain for an ideal dipole antenna $g = \frac{3}{2}$ (G=1.76 dB).

B.2 Characteristics of the half wave dipole antenna

A very widely used antenna is the half-wave dipole antenna. It is a linear current whose amplitude varies as one-half of a sine wave with a maximum at the center. It could be imagined to flow on an infinitely thin, perfectly conducting, half wavelength long wire. The advantage of a half-wave dipole is that it can be made to resonate and in this way present a zero input reactance. To obtain a resonant condition for the half-wave dipole the physical length must be somewhat shorter than a free space half-wavelength.

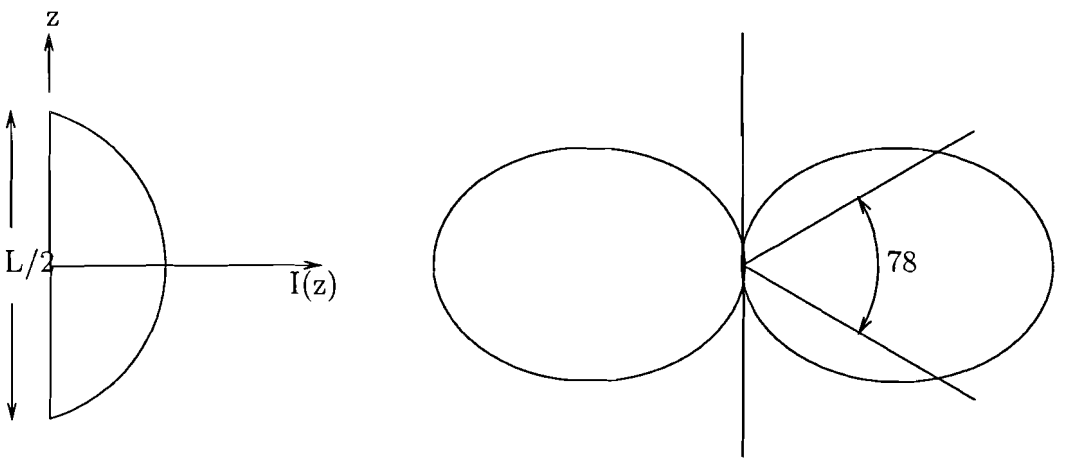

Figure B.2: (a) Current distribution of the half-wave dipole. (b) Radiation pattern

Let us again place the current along the z-axis, than the current distribution of the half-wave dipole is written as

$$I(z) = I_m \sin\left[\beta\left(\frac{\lambda}{4} - |z|\right)\right] \quad |z| \leq \frac{\lambda}{4} \tag{B.17}$$

where $\beta = \frac{2\pi}{\lambda}$. This current goes to zero at the ends and its maximum value I_m occurs at the centre as shown in Fig B.2. If we consider the half wave dipole consisting of a great number of electrical (ideal) dipoles, we can use the superpositioning theorem. Using (B.7, the far field of the half-wave dipole can be described as

$$E_\theta = \frac{j\beta Z_0 \hat{I} \sin\theta}{4\pi} \int_{-\frac{\lambda}{4}}^{\frac{\lambda}{4}} \frac{\sin[\beta(l - |z|)]}{R'} e^{-j\beta R'} dz \tag{B.18}$$

Where R' is the distance between source-point and field-point and the time dependence is not used. If we consider R to be the distance from the origin to the field-point, the following substitution can be made.

$$\frac{e^{-j\beta R'}}{R'} \approx \frac{e^{-j\beta R}}{R} e^{j\beta z \cos\theta} \tag{B.19}$$

Substitution of (B.19) in (B.18) and integration gives

$$E_\theta = \frac{jZ_0\hat{I}}{2\pi} \frac{\cos(\frac{\pi}{2}\cos\theta)}{\sin\theta} \frac{e^{-j\beta R}}{R} \tag{B.20}$$

The θ -variation of this function determines the far field pattern. This θ-variation is called the normalized electric field-pattern. The radiation pattern of a half-wave dipole (Fig B.2.b) is slightly different from the radiation pattern the ideal dipole. The half-power beamwidth pattern of the half-wave dipole is 78^0. For comparison, the half-power beamwidth of an ideal dipole is 90^0. This means that the antenna-gain of the half-wave dipole will be somewhat higher than the antenna gain of the ideal dipole.

Gain and Radiation resistance

In the same way as has been done with the ideal dipole, the antenna gain can be calculated for the half-wave dipole. Here it is sufficient to say that the antenna-gain of the half wave dipole g=1.64 (G=2.15 dB). Another important characteristic of an antenna is the radiation resistance or input impedance. If we again look at the radiated power of the antenna we find with (B.11) and (B.10)

$$P_{r,\text{dipole}} = \frac{1}{2Z_0}\int_0^{\pi}\int_0^{2\pi} |E_\theta|^2 R^2 \sin\theta \, d\theta \, d\phi \tag{B.21}$$

After substitution of E_θ and integration over ϕ we find

$$P_{r,\text{dipole}} = \frac{Z_0 \hat{I}^2}{4\pi}\int_0^{\pi} \frac{[\cos(\frac{\pi}{2}\cos\theta]^2}{\sin\theta} d\theta \tag{B.22}$$

This radiated power has to be dissipated in an equivalent resistor of R_r Ohm. If we look at the current for $z = 0$ we find for the power

$$P_{r,\text{dipole}} = \frac{1}{2}\hat{I}^2(0)R_r = \frac{1}{2}\hat{I}^2 \sin^2\frac{\pi}{2} R_r \tag{B.23}$$

From this follows for the radiation resistance of the half-wave dipole

$$R_{r,\text{dipole}} = 60\int_0^{\pi} \frac{[\cos(\frac{\pi}{2}\cos\theta]^2}{\sin\theta} d\theta \tag{B.24}$$

If we work out the integral we find the radiation resistance R_r to be 73.13 Ohm.

B.3 Characteristics of the ground plane antenna

Antennas are frequently operated in the presence of other structures. One such structure that is commonly encountered is a ground plane. A ground plane in its ideal form is infinite in extent and perfectly conducting, often referred to as *perfect ground plane.* A solid metal sheet that is large compared to the antenna size is, in most cases, well approximated as a perfect ground plane. The characteristics of the quarter-wave ground plane antenna ($\lambda/4$ monopole) can easily be deducted from the characteristics of the halve wave dipole.

A monopole is no more than a dipole divided in half at its center feed point and fed against a ground plane. Therefore, the currents and charges on a monopole are the same as on the upper half of its dipole counterpart, but the terminal voltage is only half that of the dipole. The input impedance for a monopole is therefore half that of its dipole counterpart, in other words

$$Z_{\text{in, mono}} = \frac{V_{\text{in, mono}}}{I_{\text{in, mono}}} = \frac{\frac{1}{2}V_{\text{in, dipole}}}{I_{\text{in, dipole}}} = \frac{1}{2}Z_{\text{in, dipole}} \tag{B.25}$$

where $Z_{\text{in, mono}}$ is the input resistance for a monopole. The same calculation can be made for the radiation resistance $R_{r,\text{mono}}$ of a monopole

$$R_{r,\text{mono}} = \frac{P_{r,\text{mono}}}{\frac{1}{2}\left|I_{\text{in, mono}}\right|^2} = \frac{\frac{1}{2}P_{r,\text{dipole}}}{\frac{1}{2}\left|I_{\text{in, dipole}}\right|^2} = \frac{1}{2}R_{r,\text{dipole}} \tag{B.26}$$

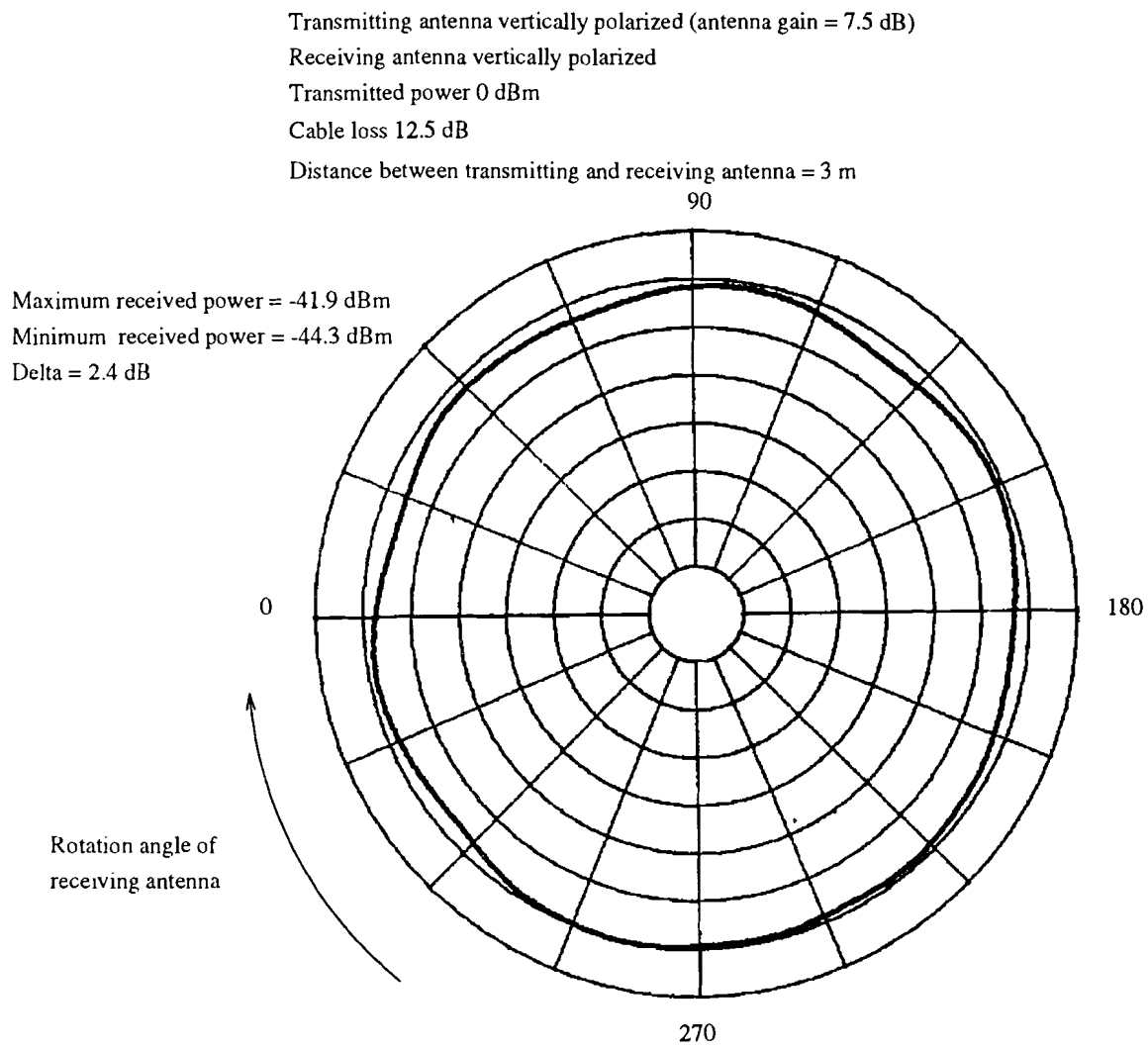

Figure B.3: Antenna diagram (xy plane) for the antenna used during the measurements.

The radiation pattern of a monopole above a perfect ground plane is the same as that of a dipole (we only observe above the ground plane). Therefore, a monopole radiates one-half of the total power of a similar dipole in free space. This means that the antenna-gain of a monopole is one-half the gain of a dipole.

B.4 Characteristics of the antenna used for the measurements

The antennas used for the measurements are of the quarter wave length type. A large metal plate was used as ground plane. This metal plate can not be assumed to be ideal. Therefore, the characteristics of the used antennas where measured in a anechoic chamber. For the transmitting antenna a Log Periodic antenna was used. The antenna characteristics of this antenna are known. We can determine the antenna gain of the receiving

antenna in the following way

$$G_r = P_{re} - P_{tr} - G_{tr} + L_c + L_{bf} \quad \text{(dB)} \tag{B.27}$$

where P_{re} is the received power, P_{tr} is the transmitted power, G_{tr} is the antenna gain of the transmitting antenna, L_C is the cable loss and L_{bf} is the basic transmission loss. The basic transmission loss for free space propagation is given by

$$L_{bf} = 20 \log \left(\frac{4\pi d}{\lambda} \right) \tag{B.28}$$

where d is the distance between transmitter and receiving antenna in meters. For $f = 763$ MHz ($\lambda = 0.393$ m) this reduces to

$$L_{bf} = 30.1 + 20 \log d \ \text{(dB)} \tag{B.29}$$

All variables filled in gives the following expression for G_r

$$G_r = P_{re} + 42.5 \tag{B.30}$$

The received power at the receiving antennas varied between -41.9 and -44.3 dBm. This means that G_r lies somewhere between -1.8 and 0.6 dB. In theory, a ideal quarter wavelength monopole with an infinitely large ground plane has an antenna gain of -0.85 dB. Figure B.4 illustrates the antenna diagram in the xz plane. It can be seen can the leakage at the bottom side (below the groundplane) is very low (30 dB down).

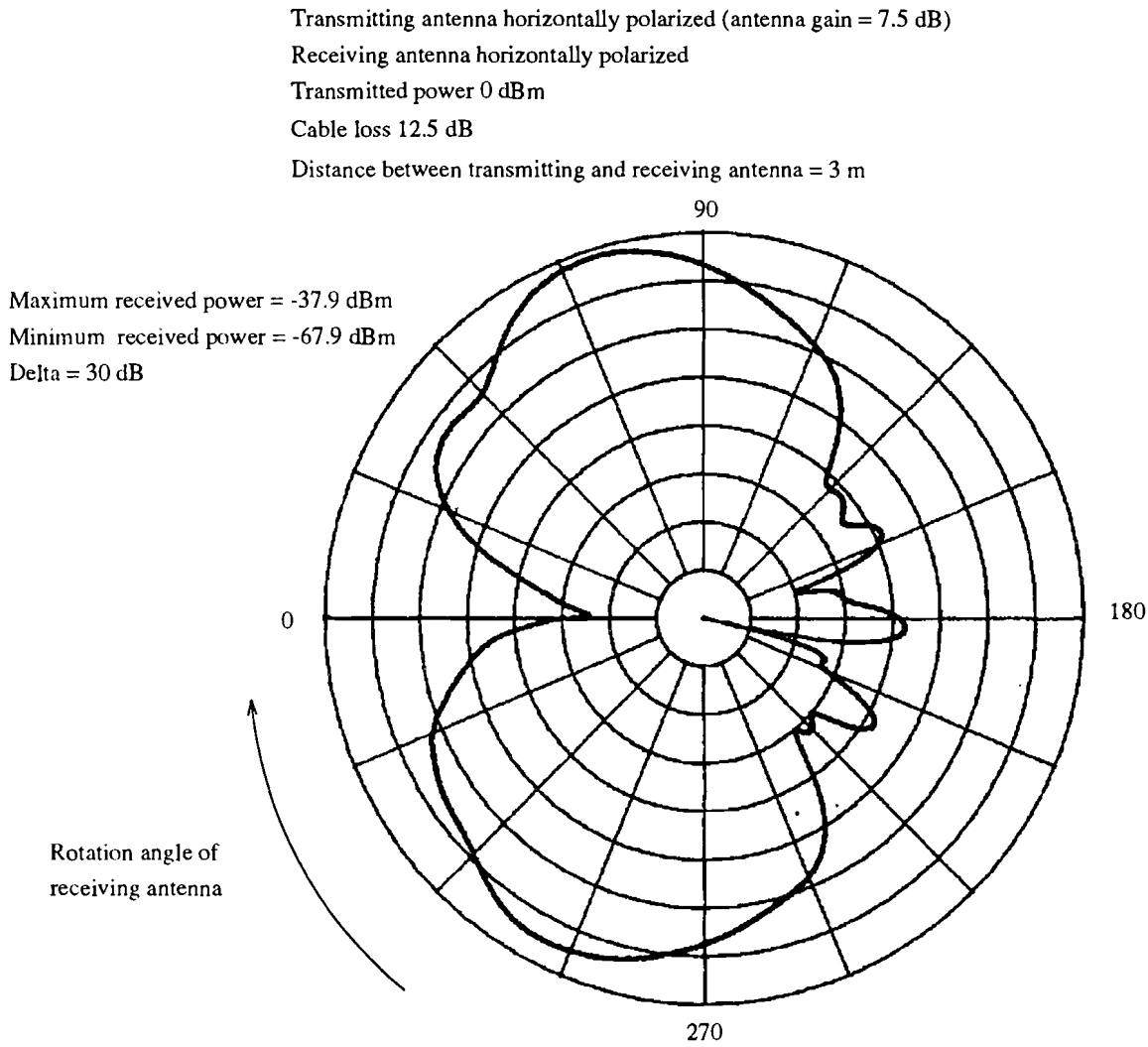

Figure B.4: Antenna diagram (xz plane) for the antenna used during the measurements.

Appendix C

The OFDM Transmitter

The dTTb project is a European project that aims to develop a (new) digital terrestrial broadcast standard that should replace the current PAL/SECAM TV. For test purposes, Philips Research Laboraties in Paris (LEP) have developed a DTTB test modem (transmitter and receiver). This modem has been installed in Eindhoven.

The transmitter is being installed at building WY of Philips Research in Eindhoven. This transmitter transmits a OFDM test signal in UHF channel 57 (758-766 MHz). The height of the transmitter antenna is about 65 meter. The UHF channel is 8 MHZ wide but the OFDM transmitter generates a power spectrum with an effective bandwidth of 7 MHz. This generated signal has a flat power spectrum so, the transmitter power is uniformly distributed over the bandwidth.

The power at the input of the transmitting antenna is 19.2 W. The antenna gain of the used transmitting antenna (Kathrein K733147) with respect to an isotropic radiator equals 15.5 dB. This means that the Effective Isotropic Radiated Power (EIRP) is 681 W.

The transmitting antenna is vertically polarized and is directed to the North/North-East and covers most of the city of Eindhoven.

Figure D.1 shows the coverage area of the antenna. The two straight lines are the -6 dB lines, and are derived from the antenna diagram of the transmitting antenna [8].

More details about the test signal are described in [8].

Appendix D

Measurement sites

Measurements where carried out in a large number of residential houses, apartment buildings and office buildings in Eindhoven:

- 18 residential houses, mostly constructed from brick or conrete or a mixture of both. The sites where scattered all through the reception area.
- 9 apartment buildings, mostly constructed from reinforced concrete. The floor number varied from 1 to 8. Reception quality in the apartment buildings depends heavily on the reception height, at high floors there is often a line-of-sight with the transmitting antenna.
- 15 office building, mostly constructed from reinforced concrete.

For a graphical overview of all measurement sites see Figure D.1.

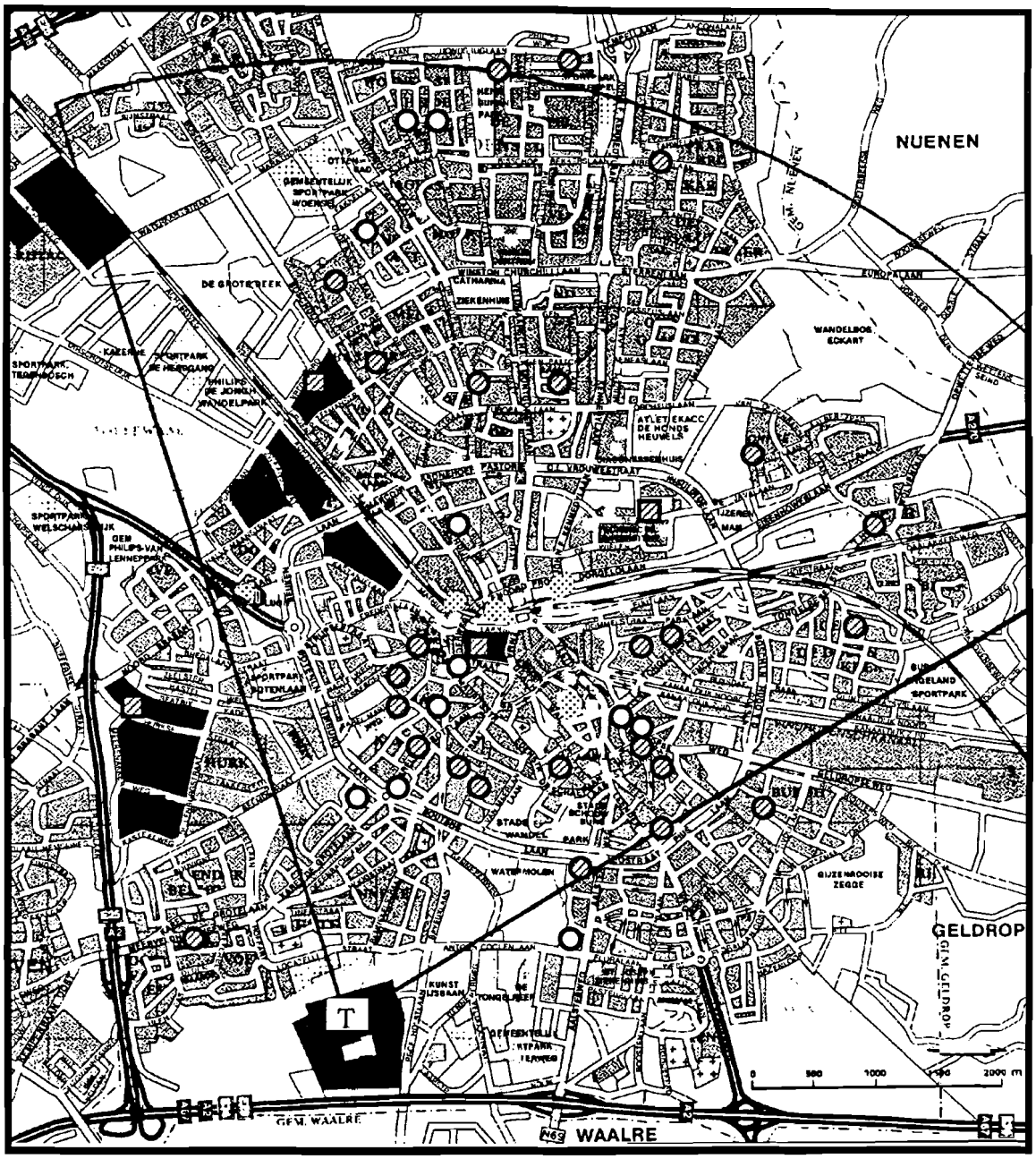

RESIDENTIAL HOUSE

APARTMENT BUILDING

OFFICE BUILDING

T TRANSMITTER LOCATION

Figure D.1: Measurement sites

Appendix E

Glossary of Notations

notation	meaning
$h(\tau)$	impulse response
$\mathcal{N}$	number of paths
$\delta(\tau)$	dirac pulse
$s(t)$	transmitted signal
$r(t)$	received signal
E_s	the energy per symbol
f_c	the carrier frequency
α	the resulting complex attenuation factor
α_i	the complex attenuation factor of a single path
γ_s	the time averaged signal-to-noise ratio per symbol
$\Phi_c(\tau)$	delay power spectrum
T_m	the multipath spread
$H(f)$	the channel transfer function
B_c	the coherence bandwidth
$\psi_{i,k}(t)$	othogonal base of signals
T_s	symbol time
T_g	guard interval time
B	bandwidth
f_s	subchannel bandwidth
N	number of OFDM subchannels
R	code-rate
B_eff	effective bandwidth
N_{eff}	effective subcarriers
λ	wavelength
L	number of antennas

notation	meaning
$E^{(t)}[\cdot]$	time average
$E^{(x)}[\cdot]$	location average
r_j	received signal at jth antenna
α_j	the resulting complex attenuation factor at the jth antenna
γ	the time averaged signal-to-noise ratio
γ_j	the time averaged signal-to-noise ratio at antenna j
$\overline{\gamma}_j$	the location average of γ_j
r_c	the combined signal
β_j	the weigthing factor of antenna j
$p_\xi(x)$	density function
$P[\xi \leq x]$	distribution function
N_0	noise power
G	gain achieved with a certain combining technique
$\overline{G}$	average gain achieved with a certain combining technique
P_{wide}	the wide-band received power of a measured OFDM spectrum
P_k	the measured power received in subchannel k
α_k	the real attenuation factor of subchannel k
P	the averaged received power per OFDM subchannel
$\overline{\gamma}_b$	the average signal-to-noise ratio per bit
Q	number of simulation runs

Appendix F

Article "Antenna Diversity for Digital Video Broadcasting"

In proceedings: IEEE first symposium on communications and vehicular technology in the benelux, October 27-28, 1993, Delft , The Netherlands.

Antenna Diversity for Digital Video Broadcasting

Johan G.W.M. Janssen*, Paul G.M. de Bot† Antoine J.M. Wijlaars†

Abstract

In the future, digital terrestrial broadcast systems in Europe will probably be OFDM-based. With indoor and portable reception of such broadcasted signals, the received signal suffers from frequency selective fading. A number of sub-channels of the OFDM spectrum may be to weak for reliable reception. A well known method of improving the performance of a system is to apply antenna diversity. Due to the indoor reception of a terrestrial signal with large delays, many fades within the bandwidth of the desired signal exist. Because of the small spatial variation of the wide-band received signal power and the many fades in the bandwidth of the signal, traditional wide-band combining will not result in much gain. In this paper we analyse the performance of antenna diversity with narrow band combining using measurements of a broadcasted OFDM signal. Combining can not only be performed on sub-channel level, but it is also possible to combine more than one channel at the same time (16, 64, 256 etc. channels).

The results show that the average gain reached with narrow band selection combining is about 5.5 dB. At locations with poor reception the gain will be even higher. With wideband selection combining an average gain of 2 dB is achieved.

1 Introduction

It is only a matter of time before the current analog television system, in Europe PAL/SECAM, will be replaced by a new terrestrial digital television system, baptized DTTB (Digital Terrestrial Television Broadcasting). This new digital system must supply a hierarchy of picture qualities, ranging from standard definition (SD) which is comparable with PAL quality via enhanced definition (ED) to high definition (HD). An example of such a system, which uses Orthogonal Frequency Division Multiplexing (OFDM), is described in [1]. OFDM is a technique to multiplex many narrow-band signals into one wide-band signal using a Fast Fourier Transform (FFT) [2]. Guard intervals are used to combat the multipath effects. With these guard intervals, OFDM is very well suited for transmission over multi-path fading channels as for example the terrestrial VHF/UHF channel [3].

A vertically polarized OFDM test signal with a bandwidth of 7 MHz is being transmitted from one of the buildings of Philips Research labs in Eindhoven. The center-frequency of the transmitted signal is 762 MHz (UHF channel 57, wavelength $\lambda = 39.4$ cm). The frequency spectrum of the OFDM signal is flat. Because of the fact that the spectrum is flat, it is very well suited for channel measurements. This signal can be received at most locations in Eindhoven.

One of the main problems in the wide-band system design is the frequency selective nature of channels like the indoor reception channel (multipath channel). The characteristics of the multipath channel are described in Section 2. Narrow-band antenna diversity as well as different combining techniques are described in Section 3. In Section 4-5 the measurements setup is discussed and the results are presented. In Section 6 the results are discussed and in Section 7 the conclusions are formulated.

2 The Multipath Channel

Consider a system where we transmit a narrow-band signal s, where $E[ss^*] = E_s$. If we transmit s over a multipath channel, the signal will reach the receiver through $\mathcal{N}$ different paths with different lengths. Each path i, $i = 0, \ldots, \mathcal{N}$-1 has its own attenuation factor a_i and propagation delay τ_i, where τ_i is assumed to be small with respect to the symbol duration. The received signal becomes $r = \sum_{i=0}^{\mathcal{N}-1} a_i e^{-j2\pi f_c \tau_i} s = \alpha s$, where f_c is the carrier frequency of the transmitted signal. In the presence of white gaussian noise n, the received signal r becomes $r = \alpha s + n$. We further assume

*Eindhoven University of Technology, Eindhoven, The Netherlands

†Philips Research Laboratories, P.O. Box 80.000, 5600 JA Eindhoven, The Netherlands

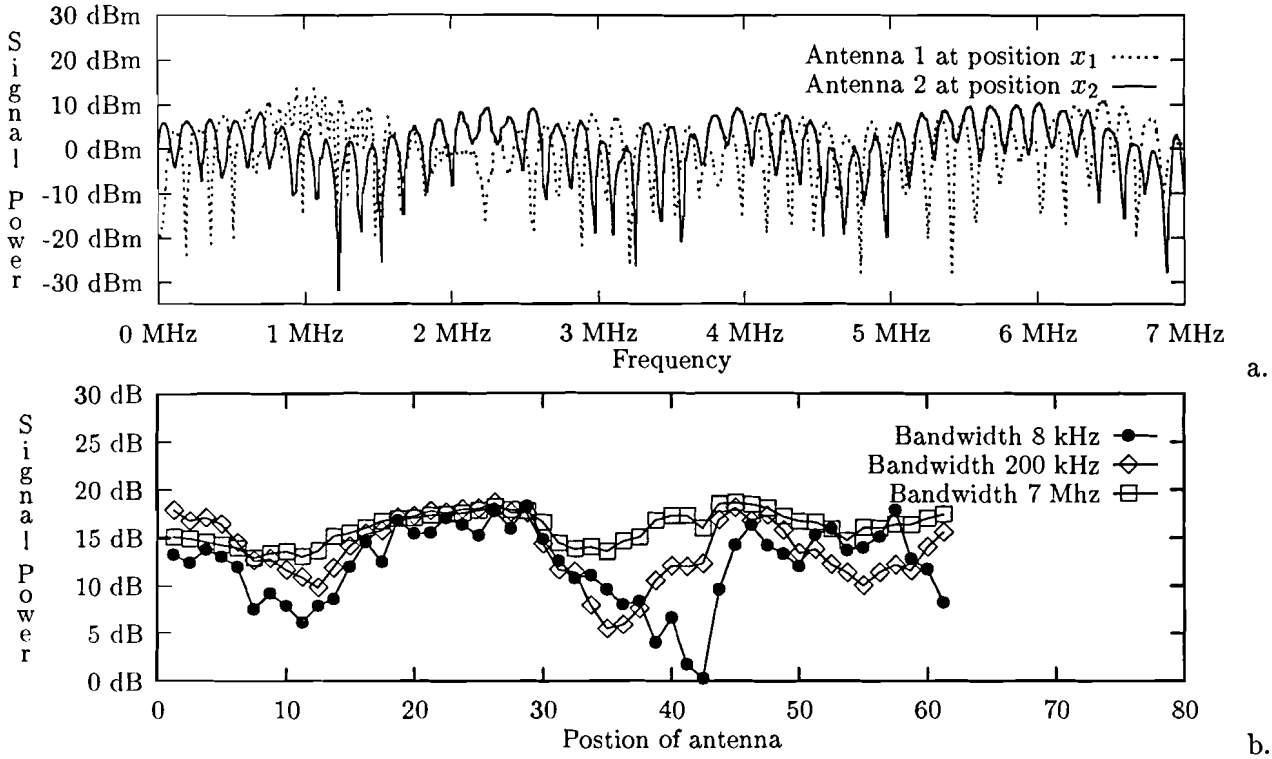

Figure 1: a. Received power spectrum at positions x_1 and x_2, $x_1 - x_2 = \lambda/2$, b. The normalised received signal strength for different bandwidths, of an original flat 7 MHz wide OFDM spectrum, as a function of the antenna position.

$E[\alpha\alpha^*] = 1$ and $E[nn^*] = N_0$.
Because the different received paths can add up destructively or constructively at a certain location, the received narrow-band signal strength is very dependent on the location of the receiving antenna (spatial fading). At specific antenna locations the received narrow-band signal can be in a deep fade and all information will be lost. The distance over which we need to shift the antenna in order to receive essentially independent signal strengths in such channels is called the coherence distance X_c. This coherence distance is usually in the order of $\lambda/2$, where λ is the wavelength of the transmitted signal.

Until now we have assumed to transmit a narrow-band signal. The OFDM signal is a wide-band signal. If we transmit the OFDM signal over a multi-path channel, the received signal suffers from frequency selectivity [4]. Therefore the complex attenuation factor α not only varies as function of the location of the antenna but α also depends on the frequency. The minimum frequency spacing over which the channel transfer function is essentially uncorrelated, is called the coherence bandwidth $(\Delta f)_c$ [4]. This coherence bandwidth is dependent on the delay spread. The longer the delay spread, the closer the spacing of the fades in the frequency domain. In a broadband situation with indoor portable reception, the coherence bandwidth can be very small (50 kHz). Figure 1a shows two received OFDM spectra with two different antennas spaced by $\lambda/2$. This figure illustrates the frequency selectivity. If we compare the two received signals, we can see that the fades occur at different frequencies.

Figure 1b shows the measured signal power as function of the antenna position for three different bandwidths. The receiving antenna was placed indoors (no line of sight with transmitter). We can see that the narrow-band received signal strength is very dependent on the antenna location. The wide-band received signal strength, on the other hand, is not very dependent on the antenna position. This averaging effect is typical for a terrestrial multipath channel.

3 Antenna Diversity

Antenna diversity at the receiver side can be used for improving the performance of a system. Commonly known and used forms of antenna diversity include spatial diversity (two or more antennas at a distance x apart), angle diversity (two or more (reflector) antennas "looking" at different angles) and polarisation diversity (two antennas with different orthogonal polarisation) [5].

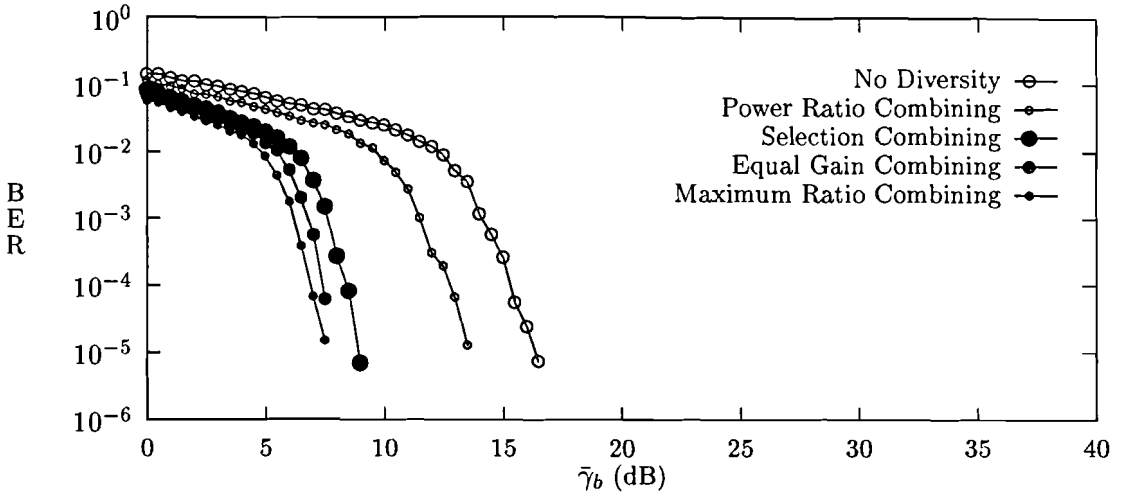

Figure 2: Performance of RS[255,223,33]-coded QPSK with $L = 2$ Antenna Diversity on an infinitely interleaved Raleigh Fading Channel.

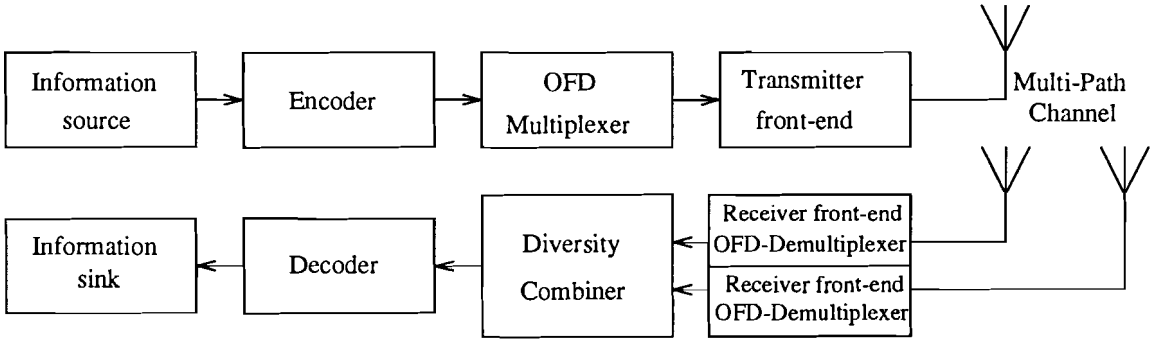

Figure 3: Implementation of the transmission scheme.

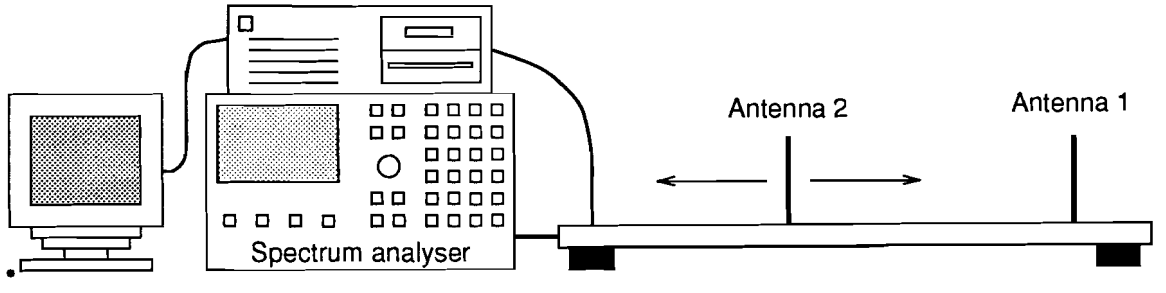

Figure 4: The measurement system.

Consider a received signal where the complex attenuation factor α is constant over the received spectrum (flat fading) but only dependent on the antenna position. One way to solve the problem of fading, is the use of spatial diversity. Consider an array of L antennas. If the antenna spacing is larger than the coherence distance X_c, the received signals at the different antennas will be uncorrelated. The received signals of all antennas need to be combined into a new signal by a combiner. We want to design a combiner that maximizes the average signal-to-noise ratio $\overline{\gamma}$ and improves the resulting distribution of the signal-to-noise ratio. On each antenna j, $j = 1, \ldots, L$, we receive the signal $r_j = \alpha_j s + n_j$, where α_j is the complex attenuation factor of the j^{th} antenna signal and n_j is the noise component of the j^{th} signal.

A combiner generates a received signal $r = \beta s + n$. We can distinguish several different combining techniques. We can simply add up all the received signals r_j. This combining technique is called linear combining. Linear combining does not improve the average signal-to- noise ratio. Assume that we can make a perfect estimate of the phase $\angle\alpha_j$ of the received signals. Now we can combine the L signals by adding them up, each signal corrected for the phase $\angle\alpha_j$. This combining technique is called equal gain combining. The optimal combining method is maximum ratio combining, where the L signals are added up, each weighted with the complex conjugate of α_j [6]. Another combining method is selection combining, where one antenna signal is processed according to a specified selection criterion. One selection criterion is to choose the antenna signal with the largest received power. In Figure 2 (taken from [7]), the performance of the different combining techniques as function of the average signal-to-noise ratio is shown with $L = 2$ antenna diversity on an infinitely interleaved Rayleigh fading channel. For RS-coded QPSK, maximum ratio, equal gain and selection combining lead to a significant performance improvement. Other combining techniques not using the phase information did not result in gain and will not be investigated any further.

Until now we have assumed that the complex attenuation factors α were constant over the received spectrum (flat fading). This is not valid for wide-band signals such as OFDM. Because of the frequency selective spatial fading and the fact that there is only a little variation in the total received wide-band power, wide-band combining will not result in much gain.

In [7], it is suggested to perform the combining for each OFDM sub-channel separately. In other words, the front-end and OFD demultiplexer needs to be implemented L fold. The outputs of the different OFD demultiplexers are fed to N combiners. Much higher gain can be achieved with this kind of narrow-band combining on a frequency selective fading channel.

An implementation of a complete OFDM transmission scheme with $L = 2$ receiving antennas is shown in Figure 3. This scheme is also used for the measurements as described in the next section.

4 Channel Measurements

The transmitted OFDM signal, discussed in the introduction, is used for the measurements. Due to multipath effects the transmitted spectrum is disturbed on its way to the receiving antenna. Using measurements of the received OFDM spectra, and simulations using these spectra, the gain of $L = 2$ antenna diversity with narrow-band combining is determined.

The measurements were carried out with the system showed in Figure 4. The computer is used as control-unit. With a little motor, antenna 2 can be moved over a distance of about 1 meter. In this way the antenna spacing is varied. The OFDM power-spectra, measured by the spectrum analyser, are sent to the computer and stored on a hard-disk for later evaluation and used in simulations. The antennas used to receive the 7 MHz wide OFDM signals, are $\lambda/4$ monopoles with a groundplane, tuned for UHF channel 57 (758-766MHz). A large metal plate is used as groundplane. Both antennas are vertically polarised. The antennas are connected to a spectrum analyser with a coaxial cable. The first experiments showed that the antenna characteristics approached those of theoretical $\lambda/4$ mono-poles with an infinitely large ground-plane [8][9].

To obtain representative results it is neccesary to measure the OFDM spectrum at many different locations. The locations were taken all over Eindhoven. Measurements where carried out in a large number of office-buildings, residential houses and apartment buildings within the range of the transmitter. Multiple measurements per location were carried out. In residential houses, for example, measurements where carried out in the living room, kitchen and other rooms that were reachable with the measurement setup. In the office buildings many measurements were carried out in different rooms and floors [8].

During a measurement run, the setup was placed

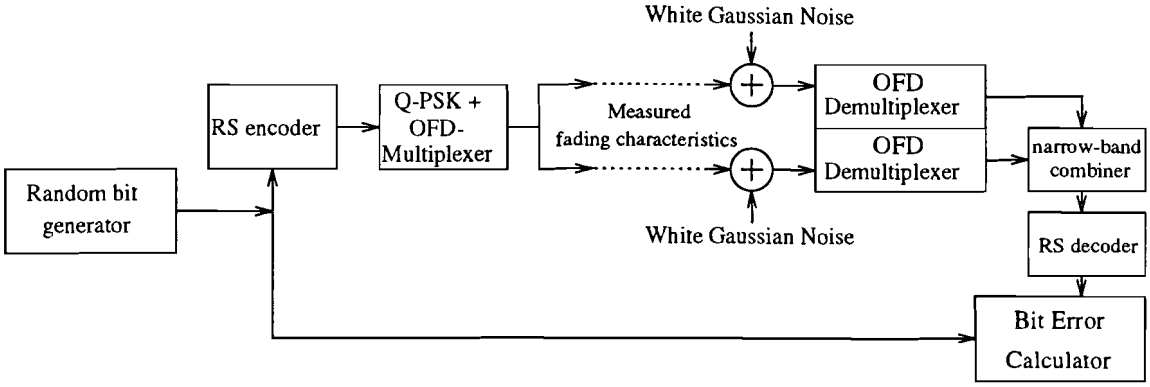

Figure 5: Simulation of narrow-band combining.

at a fixed position, while antenna 2 was moved to vary the distance between the two antennas. The initial spacing of the two antennas was always 10 cm ($\approx \lambda/4$). During one measurement run, 50 spectra received from each antenna were measured and sent to the computer. After a spectrum was read, antenna 2 was moved each time over a distance of 1.25 cm ($\lambda/32$). After 50 measurements the distance between the antennas was 72.5 cm. The measurements showed that under stationary conditions the two antennas did not influence each other, so antenna 1 received 50 identical frequency spectra.

During a period of three weeks, measurements were carried out at 40 different locations. At each location, a number of 3 to 8 measurement runs were carried out. This gave a total of approximately 200 measurement runs. One month after the measurements were finished, a few locations were visited again to verify the earlier acquired data.

5 Simulations of combining techniques

In this section, results are presented showing the difference in performance between several narrow-band and wide-band combining techniques. The results were derived from computer simulations. Figure 5 shows how the computer simulations are carried out. Each block in Figure 5 is a subprogram that performs the action desired. Initially bits are generated randomly. The generated bits are encoded in a Reed Solomon encoder using a RS[255,223,33] code. Each Reed Solomon block consists of 255 bytes. Each byte is allocated to a specific OFDM subchannel. When we use four of these code-blocks $4 \times 255 = 1020$ sub-channels will be occupied. During the simulation, no frequency interleaving was applied between the channels that belonged to a certain block. In [8], simulation results for different frequency interleaving depths are presented. The encoded bits are converted to a QPSK constellation and multiplexed into an earlier discussed OFDM signal. The measured OFDM signal with a bandwidth $B = 7$ MHz is divided into 1020 sub-channels. The sub-channel spacing becomes $f_s = B/1020 = 6.8$ kHz.

The spectra measured at the different locations were used as fading characteristics in the simulations. Each received OFDM sub-channel has its own received signal strength. By normalising the wide-band received average signal power, an attenuation factor for each OFDM sub-channel can be calculated. Each OFDM sub-channel will now be disturbed by a different attenuation factor. Because the measured spectra had no phase component, the attenuation factor used to disturb the simulated OFDM signals is a real value. Since maximum ratio combining and equal gain combining use some kind of phase recovery (coherent detection) to combine the different signals, we don't need a phase component (presuming perfect recovery). White Gaussian Noise is added to the disturbed signal. The two received signals are combined at sub-channel level and generate a new signal that will be QPSK-demodulated and RS-decoded, so we can calculate the final bit error rate (BER). If we keep in mind that for each k^{th} sub-channel $r_k = \alpha_k s_k + n_k$, we can define a signal-to-noise ratio γ_k for each different sub-channel. $\gamma_k = \frac{|\alpha_k|^2 E_s}{N_o}$. The noise power level N_0 can be varied. Now it is possible to calculate the BER as function of the mean signal-to-noise ratio per transmitted bit, $\overline{\gamma}_b = E_b/N_0$, where E_b is the energy per information bit.

In Figure 1a we showed two different spectra received at the same location with an antenna-spacing of $\lambda/2$. We can use these two spectra to simulate and calculate the bit error rate of differ-

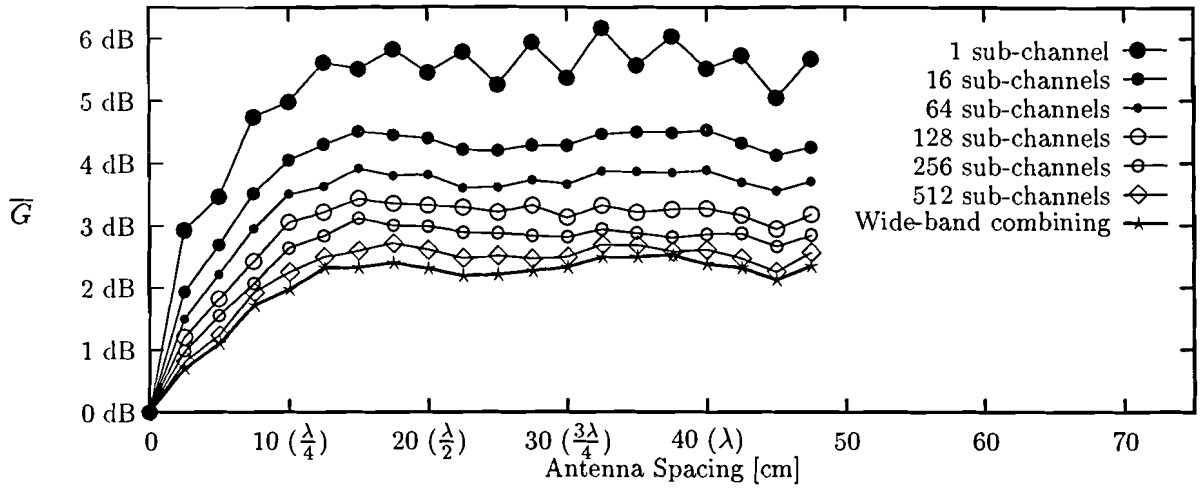

Figure 7: Simulation results for a coded OFDM scheme for 2 antenna selection-combining with a decreasing combining resolution, as function of the antenna spacing. The wavelength of the received signal is 39.4 cm (BER = 10^{-4}).

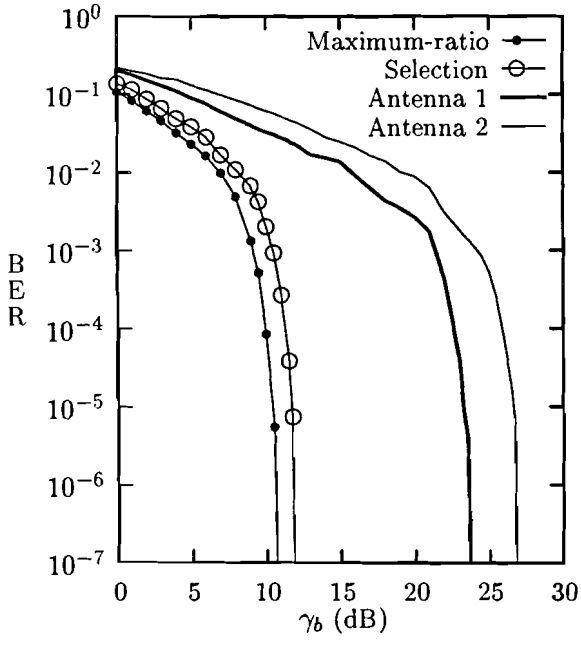

Figure 6: Simulation results for a coded OFDM scheme for different narrow-band (2 antennas) combining techniques and results with no combining.

ent combining techniques as function of the signal to noise ratio. Figure 6 shows these results. Both maximum-ratio and selection combining are simulated. For bit error rates smaller than 10^{-4}, maximum-ratio combining performs 1 dB better than selection combining, and selection combining performs 13 dB better than no combining in this particular case. The two curves on the right are the simulation results for the received signals, achieved without antenna diversity. We can define the gain G as the performance improvement of the system, achieved with selection combining. For this particular case $G = 13$ dB. Of course this is only one example at one location at one antenna distance, for which the gain obtained with narrow-band combining is very high. We are more interested in a linear average value of G ($\overline{G}$) were we can see the performance difference between narrow-band combining and traditional (wide-band) combining. We also like to investigate if there is an optimum antenna spacing. In order to reduce the complexity of a receiver, it is advantageous to minimise the subdivision of the wideband spectrum before combining. If the coherence bandwidth $(\Delta f)_c$ is much larger than the bandwidth of a single OFDM subchannel, it might very well be possible that combining with more than one sub- channel is as effective as combining per individual sub-channel. We have already mentioned that each measurement run consisted of 50 spectra for each antenna. If we want to carry out simulations with these spectra, we can use the measured spectrum of antenna 1 and combine it with any of the 50 measured spec-

tra of antenna 2. Another possibility is to combine the received spectra of antenna 2 at those 50 location mutually. This leads to 50 × 49 more useful combining simulations for each measurement run. Because the simulations are very time-consuming, not every measured spectrum was taken into account. From the complete set of 50 spectra in each measurement run, only 25 were used.

If the combining bandwidth is larger than the sub-channel spacing, the attenuation factor α is not constant any more and maximum ratio combining can not be simulated anymore. For this reason only the performance of selection-combining is simulated. For each sub-channel or number of sub-channels the strongest signal is selected. If we combine per sub- channel, the signal with the largest amplitude is selected, but if we combine with more than one sub-channel, the mean power over these sub-channels is calculated and the ones with the largest mean power are selected. Figure 7 shows the simulation results, giving a mean value of G over all locations.

6 Discussion

A number of things can be derived from these results. First we see that the antenna spacing is of importance. If the antenna spacing is larger than $\lambda/3$, $\overline{G}$ becomes constant. We also see that the combining bandwidth is of importance. If we compare the performance of narrow-band combining (1 sub-channel) with wide-band combining (1024 sub- channels), we see that on average narrow-band combining performs about 3.5 dB better than wide-band combining. If we would consider only locations far away from the transmitter, at the ground floor with absolutely no line of sight component, the performance gain of narrow-band combining compared with wide-band combining is much larger. In other words, at locations with poor reception conditions, the gain of narrow-band combining, compared to wide-band combining, tends to be larger. Numerical results will be presented in [8].

From the decrease in performance, when more sub-channels are combined at the same time, it can be derived that the spatial fading of the received spectra decreases if we look at the mean power of an increasing frequency-band. Wide-band combining also results in some gain. This means there will still be some wide-band spatial fading (flat fading). If we calculate the average received narrow-band power fluctuation over a distance λ, at every measurement location, we find this to be 16 dB.

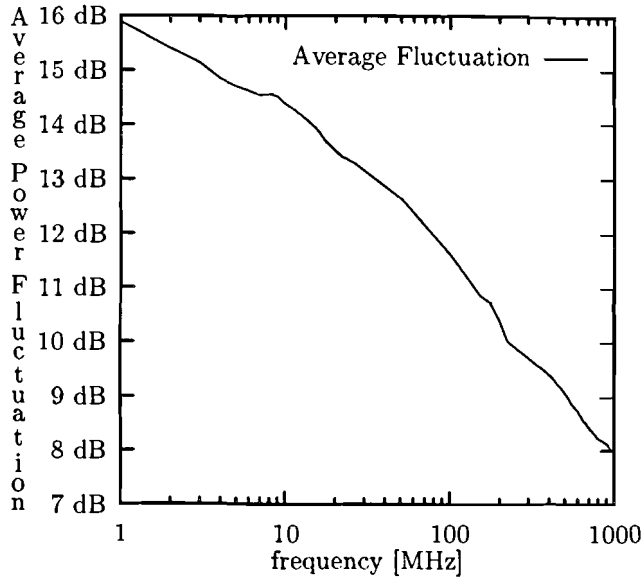

Figure 8: Average power fluctuation as a function of the combining bandwidth.

If we increase the bandwidth over which we calculate the average received power fluctuation, we have the results of Figure 8. We can see that the average wide-band power fluctuation of the OFDM spectrum is 8 dB lower than the average narrow-band power fluctuation. This difference is an indication for the extra gain that can be accomplished with narrow-band combining compared to wide-band combining.

The results shown in Fig 7 only give information about the mean value G. It is also interesting to know how the actual gain is distributed over the different measurements. We can make a gain distribution function. Figure 9 shows the distribution of the gain achieved with 1 sub-channel combining. The results from measurements where the antenna spacing was smaller than $\lambda/3$ were not taken into account. One striking item in the results of Figure 9 is the fact that locations exist, where no gain is obtained with narrow- band selection-combining. This can be easily explained. If we receive two different OFDM power-spectra at two different locations, narrow-band selection combining selects for each sub- channel the strongest one. If one received spectrum is entirely stronger than the other one, selection combining will select every sub-channel from the stronger one. The gain reached in comparison with that spectrum is then of course 0 dB.

From this distribution we can calculate the probability that the gain exceeds a certain value y ($P[G > y]$). Let us consider the case of narrow-band combining. We found the average gain to

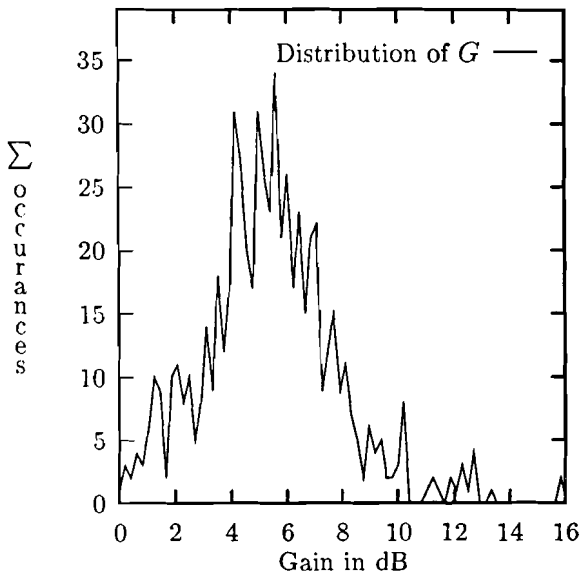

Figure 9: Distribution of G, using sub-channel selection combining for a coded OFDM scheme.

be 5.5 dB. If we calculate $P[G > 5.5 \text{ dB}]$, we find this to be $P[G > 5.5 \text{ dB}]=0.34$. We can say that narrow-band combining exceeds the mean gain reached with narrow-band combining in 34% of the cases.

7 Conclusions

We have determined the performance of selection-combining using different combining bandwidths on measured frequency selective channels. Wide-band selection combining improves the performance with 2 dB with respect to no antenna diversity. Narrow-band combining, on the other hand improves, on average, the performance with 5.5 dB with respect to no antenna diversity. At locations with poor reception conditions the gain of narrow-band combining is even larger.

References

[1] P.G.M. de Bot C.P.M.J. Baggen, A. Chouly, and A. Brajal. An example of a multi-resolution digital terrestrial TV modem. In *Proc. Int. Conference on Communications*, pages 1785–1790, Geneva, Switzerland, May 1993.

[2] S.B. Weinstein and P.M. Ebert. Data transmission by frequency-division multiplexing using the discrete fourier transform. *IEEE Trans. Communications*, COM-19(5):628–634, October 1971.

[3] M. Alard and R. Lassalle. Principles of modulation and channel coding for digital broadcasting for mobile receivers. *EBU Review*, (224):168–190, August 1987.

[4] J.G. Proakis. *Digital Communications.* McGraw-Hill, Singapore, second edition, 1989.

[5] W.C. Jakes. *Microwave Mobile Communications.* Wiley, 1974.

[6] D.G. Brennan. Linear diversity combining techniques. *Proc. IRE*, 47(6):1075–1102, June 1959.

[7] P.G.M. de Bot. Antenna diversity for OFDM systems. In *Proc. Symp. on Information Theory in the Benelux*, pages 244–251, Veldhoven, The Netherlands, May 1993.

[8] J.G.W.M. Janssen. Antenna diversity for digital video broadcasting. Master's thesis, Eindhoven University of Technology, Eindhoven, The Netherlands, November 1993. (In Preparation).

[9] W.L. Stutzman and G.A. Thiele. *Antenna theory and design.* Wiley, New York, 1981.